國立臺灣大學生命科學院生化科學研究所

碩士論文

Graduate Institute of Biochemical Sciences

College of Life Science

National Taiwan University

Master Thesis

# 建立影像式搜索策略
# 鑑別參與特定性細胞自噬的去泛素化酶

# An image-based screening strategy to identify deubiquitinases in selective autophagy

陳君瑋

Chun-Wei Chen

指導教授：楊維元 博士

Adviser: Wei Yuan Yang, Ph.D.

中華民國 106 年 7 月

July, 2017

doi:10.6342/NTU201704022

# 國立臺灣大學碩士學位論文
# 口試委員會審定書

論文中文題目: 建立影像式搜索策略鑑別參與特定性細胞自噬的去泛素化酶

論文英文題目: An image-based screening strategy to identify deubiquitinases in selective autophagy

本論文係 陳君瑋 君(學號 R04B46010)在國立臺灣大學生化科學研究所完成之碩士學位論文，於民國 106 年 7 月 25 日承下列考試委員審查通過及口試及格，特此證明。

口試委員：

_____(簽名)(召集人)

_____

_____(指導教授)

# 誌謝

兩年的碩士班生活，只有「充實」能夠形容。第一年修課與實驗雙管齊下的緊湊步調，與第二年實驗、全所進度報告與畢業論文的忙碌日子，這兩年來，自己似乎也成長了一些。

首先要感謝楊維元老師，在六月時還願意收我當碩士班學生，讓我能在七月時就能順利到實驗室學習。無論我的疑問是多麼基本、實驗結果是多麼粗糙，楊老師總是很有耐心、不厭其煩的與我討論，並指引我往不同方向思考，從這些 trouble shooting 的過程中，我學習到了解決問題的態度與方法，相信這是在各領域中皆為非常重要的技能，受用無窮。兩年中，我累積了不少顯微鏡或是影像軟體相關的知識與經驗，感謝楊老師給予我機會可以親自操作貴重儀器，甚至參與維修的過程，這是不可多得的機會！

另外，我也要感謝實驗室的成員：最初苑萍的實驗帶領，珮柔、弘祥、柏樺在 cloning 方面的協助，項詒、元平在實驗討論上的腦力激盪與口試前給予我許多建議，聖捷、桑淳、正偉在實驗相關大、小事上的協助。

最後，非常感謝陳光超老師與黃馥老師，在百忙之中撥冗擔任我的口試委員，不吝提出許多的建議，讓我對於如何將這個題目做得更好，有了更多不同的刺激思考。感謝一路上所有幫助過我的人們，碩士班只是個中繼站，我會繼續努力朝夢想邁進！



doi:10.6342/NTU201704022

# 摘要

細胞自噬 (autophagy) 是一種細胞內的自我分解機制，調控細胞中物質的去與留，分解後並加以循環利用。需要被清除的物質會被自噬小體 (autophagosome)包覆後與溶酶體 (lysosome)結合，進而被溶酶體中的水解酵素分解。在分類上，細胞自噬可以由所吞噬的物質之特定性，而分成非特定性細胞自噬與特定性細胞自噬(nonselective and selective autophagy)。在特定性細胞自噬的過程中，特定的胞中物質，例如：受傷的胞器，會被泛素(ubiquitin)標定，進而被特定性細胞自噬受器(selective autophagy receptors) 辨識而形成自噬小體進行吞噬與分解。泛素在這個過程扮演了重要的角色；因此，去泛素化酶(deubiquitinases, DUBs) 在調控這個過程中也是不可或缺。在其中一種特定性細胞自噬，胞器自噬(organellophagy) 中，有部分參與其中的去泛素化酶已經被發現，他們去除標定在將被清除的胞器上的泛素，而抑制了胞器自噬的產生，但也尚有許多參與胞器自噬的去泛素化酶尚未被發掘。先前的研究有利用影像結果找尋去泛素化酶，但其方法並非使用大量、系統化的地毯式搜尋，難免會有漏網之魚。因此我們想要發展出一套以影像為主的搜索策略，在人體近一百種的去泛素化酶中，搜尋在胞器自噬中擔任負調控角色的去泛素化酶。

這套策略假設當目標去泛素化酶過度表現時，標定在受傷胞器上的泛素將會被去泛素化酶切除進而抑制胞器自噬的進行。為了使這套策略能夠系統化搜尋目



doi:10.6342/NTU201704022

標，我們首先建立了接上增強型綠色螢光蛋白(EGFP)的去泛素化酶質體庫，並將各質體一一表現於海拉細胞(HeLa cells) 中，並以光破壞的方式誘導特定的胞器自噬產生。接著利用免疫螢光染色(immunofluorescence) 標定出泛素與特定胞器的位置，並利用 ScanR 影像分析軟體計算每個細胞中的去泛素化酶的表現量與泛素標定在特定胞器上的面積，此二參數應該呈現負相關；也就是當目標去泛素化酶的表現量越高，泛素標定在特定胞器上的面積就越低。這個搜索策略可以只計算在特定胞器上的泛素(而非整個細胞中的泛素)；而且由於基因轉染的效率(transfection efficiency)因各個細胞而異，因此以單一細胞為單位，可以在一盤細胞中得到不同的去泛素化酶的表現量，便可由量化分析比較不同去泛素化酶表現量下，泛素標定在特定胞器上的面積。

我們所設計的影像式搜索方法首先由目前了解較詳細的粒線體自噬(mitophagy) 來測試其可行性。我們將已知會抑制粒線體自噬去泛素化酶USP30 表現於海拉細胞中進行測試，確定這個策略是可行的，不過仍有一些問題存在於控制組的實驗結果中，需要進一步的改正。同時，我們也準備了材料，欲將此策略應用在其他種胞器自噬中。質體庫目前已經建立了 27 個去泛素化酶質體，並且在目前了解不多的溶酶體自噬中測試了 10 個去泛素化酶，其中兩個有可能是目標，需要進一步的檢測才能確定。總而言之，我們所建立的影像搜索方法經過改正一些問題後，相信可以應用在鑑定抑制胞器自噬的去泛素化酶過程中。

**關鍵詞:** Selective autophagy, organellophagy, deubiquitinases, ubiquitin, ScanR.



doi:10.6342/NTU201704022

# Abstract

Autophagy is an intracellular digestion mechanism, termed as “self-eating” processes in quality control of cellular components. Autophagy can be categorized as nonselective and selective autophagy by the specificity of the targeted cargo, which is engulfed by autophagosomes and degraded by fusion of lysosomes. In selective autophagy, specific cellular components, such as organelles, are targeted by ubiquitin (Ub), providing a recognition by selective autophagy receptors for autophagosome formation. Since ubiquitination plays an important role in the targeting of substrates for selective autophagy, especially organelle-autophagy, the deubiquitinases (DUBs), which oppose ubiquitination, can be a key factor for suppressing organelle-autophagy. However, which DUBs are involved in organellophagy remains partially unidentified. In addition, previous studies utilize images in aid of identifying DUBs in selective autophagy, but not in a systematic and statistical ways. Therefore, the goal of the study is to establish an image-based screening strategy to robustly identify which DUBs regulate autophagic organelles turnover from over a hundred DUBs within human genome.

The assumption underlying this strategy is that ubiquitination of damaged organelle will be suppressed by the overexpression of the DUBs that regulate organelle autophagy. To enable the strategy systematically, DUBs were first cloned into EGFP vector and overexpressed within HeLa cells. To clearly observe the organelle autophagy in cells, the



doi:10.6342/NTU201704022

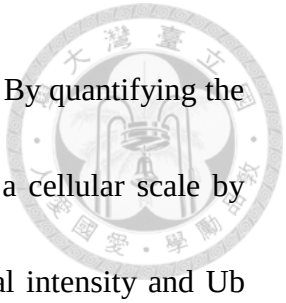

dye-labeled organelles were specifically damaged by light induction. By quantifying the Ub signal on the damaged organelles with immunofluorescence in a cellular scale by ScanR analysis software, the correlation between EGFP-DUB signal intensity and Ub signal area should be negative with the overexpression of the DUB candidates. This strategy can not only quantify the ubiquitination specifically on the damaged organelles cell by cell, but also acquire different DUB expression level in each cell due to the transfection efficiency.

This image-based screening strategy was first examined through parkin-mediated mitophagy, and one of the known DUBs for natively regulating parkin-mediated mitophagy, USP30, was tested in the assays. However, the problem in the EGFP control groups remained to be revised. Meanwhile, we prepared for applying the assay to identify the DUBs that regulate autophagic turnover of other types of organelles. So far, 27 DUBs were prepared, with 9 of them testing in lysophgy, and one DUB in Golgiohagy. There were 2 candidates showed in the lysophagy testing, and further screening need to be done. To sum up, the image-based screening strategy can become a powerful method after validation.

**Key words:** Selective autophagy, organellophagy, deubiquitinases, ubiquitin, ScanR



doi:10.6342/NTU201704022

# Contents



doi:10.6342/NTU201704022

doi:10.6342/NTU201704022

doi:10.6342/NTU201704022

# Contents of Figures and Tables



doi:10.6342/NTU201704022

doi:10.6342/NTU201704022

# Introduction

Autophagy is an intracellular digestion mechanism, termed “self-eating” processes, which can be categorized into several types through morphology of processes or specificity of cargoes (Okamoto, 2014; Shaid et al., 2013). Three modes of autophagy are defined through morphological distinction: macroautophagy, microautophagy, and chaperone-mediated autophagy (CMA) (Galluzzi et al., 2017; Kraft et al., 2010; Okamoto, 2014). In macroautophgy, the cellular components are surrounded by isolation membranes, and the isolation membranes fuse to further form autophagosome. Finally, with the fusion of lysosome and autophagosome, the engulfed components are degraded into small molecules by hydrolytic enzymes in lysosomes (Xie and Klionsky, 2007). While in microautophagy, by infolding the membrane of lysosomes, the cargos are directly engulfed by lysosome and digested by hydrolase. Different from others, CMA does not require membrane invaginations to engulf cargos for delivering to lysosomes, but the translocation complex on the membrane of lysosome assists the cargos to attach the lysosomal membrane and be degraded (Galluzzi et al., 2017).

On the other hand, by the selectivity of the targeted cargo, autophagy can be differentiated into non-selective and selective autophagy. Upon nutrient destitution (e.g. starvation), cellular constituents are recycled globally by non-selective autophagy to



doi:10.6342/NTU201704022

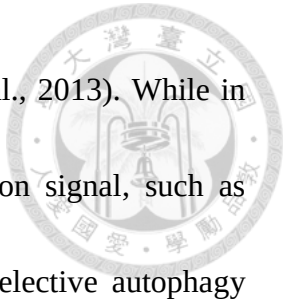

catabolize components for overcoming adverse situation (Shaid et al., 2013). While in selective autophagy, specific substrates with labeling of degradation signal, such as protein aggregates, organelles and pathogens, are recognized by selective autophagy receptors, and engulfed by autophagosomes (Shaid et al., 2013). In this study, we focus on the mechanisms in selective autophagy of organelles, termed organellophagy, since organelles are crucial elements in maintenance of cell survival and metabolism in eukaryotes (Okamoto, 2014). The malfunction of organelles can cause diseases, such as cancers and neurodegenerative diseases (Magraoui et al., 2015). As a result, understanding the mechanism of the turnover of organelles is important.

The degradation signal in selective autophagy, such as ubiquitin (Ub), reveals the specificity in degradation. Known for involving in the proteasomal-degradation pathway, Ub signal also plays an important role in selective autophagy (Kirkin et al., 2009). For example, the selective autophagy receptors can recognize the ubiquitinated organelles, and connect them to autophagosomal membranes in organellophagy, which Ub signal acts as a fate-deciding factor for organelles (Khaminets et al., 2015). In the regulation of ubiquitination, the cascade processes involve enzyme E1 (activation), E2 (conjugation) and E3 (ligation) to attach Ub chains on substrates (Reyes-Turcu et al., 2009). In contrast, deubiquitinases (DUBs) can oppose ubiquitination by trimming the Ub chains.



doi:10.6342/NTU201704022

Approximately 600 E3 ligases and a hundred DUBs are encoded by human genome (Komander et al., 2009; Reyes-Turcu et al., 2009), but which are responsible for the homeostasis of different organelles remains unclear. Accordingly, we aim to identify the unknown DUBs in organellophagy.

DUBs can be grouped into five families: ubiquitin C-terminal hydrolases (UCH), ubiquitin-specific proteases (USP or UBP), ovarian tumor proteases (OTU), Josephins (MJD) and JAB1/MPN/MOV34 metalloenzymes (JAMMs or MPN+). Apart from JAMM/MPN+ family members, which are zinc metalloproteases, the other four families of DUBs are Cys proteases (Clague et al., 2012). There are various functions of DUBs, such as maintaining Ub homeostasis, rescuing substrates from degradation, stabilizing protein, and adapting Ub linkage forms. Here we focus on the DUBs responsible for retrieving damaged or aged organelles form degradation. So far, mitophagy, ribophagy, pexophagy and lysophgy are organellophagy that has been reported in relation of Ub for regulating their homeostasis (Anding and Baehrecke, 2017; Khaminets et al., 2015; Okamoto, 2014). In addition, the DUBs that involve in the turnover of organelles have been mainly described in mitophagy.



doi:10.6342/NTU201704022

Selective autophagy of mitochondria, termed mitophagy, is vital in maintaining cellular homeostasis (Lemasters, 2005). Mitochondria is an energy generation center for generating ATP, along with calcium balance and programmed cell death (Nunnari and Suomalainen, 2012). Disorder and damage in mitochondria lead to serious diseases, for example, Parkinson's disease, a neurodegenerative disorder related to degeneration of dopaminergic neurons (Valente et al., 2004). Thus, the quality control of mitochondria in cells is critical, and the parkin-mediated mitophagy is the best studied pathways (Anding and Baehrecke, 2017). Upon mitochondrial depolarization, PTEN-induced putative kinase 1 (PINK1) phosphorylates the ubiquitin-like (Ubl) domain in N-terminal S65 of parkin, an E3 ligase (Kondapalli et al., 2012; Okatsu et al., 2013). The pS65 activate parkin, in aid of autoubiquitination with the pSer65 Ub chains by PINK1, which helps the active parkin recruit to damaged mitochondria (Okatsu et al., 2013). In the process, PINK1 serves a positive feedback for damaged mitochondria clearance by mitophagy (Koyano et al., 2014).

Since Ub signals play an important role in parkin-mediated mitophagy, the DUBs should be involved in regulation of the processes. Several DUBs linked to mitophagy have been found: USP8, USP15, USP30, USP35 (Dikic and Bremm, 2014; Magraoui et al., 2015). In the study by the group of Edward A Fon (Durcan et al., 2014), they screened



doi:10.6342/NTU201704022

for DUBs, for effecting on parkin recruitment to carbonyl cyanide 3-chlorophenylhydrazone (CCCP)-induced damaged mitochondria, through RNAi knockdown in U2OS cells expressing GFP-parkin. They found that knockdown of USP8 showed delayed parkin recruitment to damaged mitochondria, and also increased accumulation of ubiquitinated parkin because of K6-linked Ub conjugates on parkin. The main finding of the study was that USP8 deubiquitinated parkin by eliminating K6-linked Ub chains from parkin in quality control of mitochondria. Another observation (Cornelissen et al., 2014) utilized tandem affinity purification coupled with mass spectrometry to identify proteins interacted with parkin in HEK293 cells overexpressing His6-Flag-parkin. They found USP15 and showed that this DUB opposed parkin-mediated mitophagy, which impacted the mitochondrial ubiquitination without affecting parkin ubiquitination and parkin translocation to damaged mitochondria. Also in 2014, a study illustrated that USP30 antagonized parkin-mediated mitophagy (Bingol et al., 2014). They established a Flag-tagged human DUBs cDNA library, and overexpressed individual DUB along with GFP-parkin in cell lines to calculate the loss of mitochondria upon CCCP-induced mitochondria depolarization. Overexpression of USP30 in cells showed rescued mitochondria signal under CCCP treatment. In the further study by the same group, the authors demonstrated that parkin added K6, K11 and K63 linked Ub chains on damaged mitochondria. In addition, USP30 selectively removed K6 and K11



doi:10.6342/NTU201704022

Ub chains on mitochondria, regulating the homeostasis of mitochondria. Last but not least, USP35 was also reported for delaying parkin-mediated mitophagy (Wang et al., 2015). The authors built a GFP-tagged Human DUBs cDNA library, and expressed each DUB in COS7 cells to observe the localization of DUB. They picked USP30 and USP35, which showed mitochondria localization, for further mitophagy quantification assay testing. In the assay, they first established a reporter, mCherry-mGFP-SYNJ2BP (synaptojanin 2 binding protein), to which localized the mitochondrial outer membranes, to detect the percentage of mitochondria in lysosomes. The mGFP signal would be quenched in lysosome but mCherry signal would remain. Therefore, by quantifying the area of mitochondria showing only the mCheery signal, the percentage of mitochondria in lysosomes, that is, mitophagy ratio, can be determined.

Although many DUBs have been identified in mitophagy, there is little that we know about DUBs in other kinds of organellophagy. As a result, we aim to establish a general screening strategy for systematically identifying DUBs in selective autophagy, especially organellophagy. As mentioned, the screening methods for DUBs in mitophagy are mostly based on the protein localization, or the occurrence of organellophagy upon expressing or knockdown of individual DUB (Bingol et al., 2014; Durcan et al., 2014; Wang et al., 2015). To sum up, the screening assays in the previous studies are mainly image-based.



doi:10.6342/NTU201704022

In addition, the mechanisms of other kinds of Ub-related organellophagy are not well studied as mitophagy, such as, the E3 ligases are still unknown in lysophagy, thus increase the screening difficulties. Accordingly, we establish an image-based screening strategy for identifying DUBs in selective autophagy by detecting Ub recruitment on damaged organelles upon overexpressing individual DUB in HeLa cells.

We assumed that ubiquitination of damaged organelles would be suppressed by the overexpression of the DUBs that regulate organellophagy. To systematically operate the strategy, the N' terminal EGFP–tagged DUBs cDNA library was built for expressing in HeLa cells. To establish the screening priority, the DUBs on the candidate list, which was from the mass spectrometry data of lysosome related proteins form our lab member Yuan-Ping Chu, were the references for priority. Meanwhile, the cellular localization of the DUBs was also a criteria for screening, which similar distribution to specific organelles can be a sign for being a candidate. Previous studies selected the possible DUBs based on localization information. For example, USP21 showed a cytoskeleton distribution, and was further found being a regulator of centrosome and microtubule (Urbé et al., 2012).

Along with drugs or specifically organelle-bound photosensitizer with light-activated to damage the organelles (Fabris et al., 2001; Hsieh et al., 2015; Hung et al.,



doi:10.6342/NTU201704022

2013; Narendra et al., 2008), organellophagy can be induced. By quantifying the Ub signal on the organelles with immunofluorescence in a cellular scale, the correlation between EGFP-DUB expression level and Ub recruitment onto damaged organelles can be a criteria for screening. For gaining more cells for quantification, the images were montaged by scanning an area of the sample. Under the assumption, the correlation in the results of overexpressing DUBs that regulate organellophagy should be negative, compared with the correlation in the results of overexpressing DUBs not for specific organellophagy or EGFP vector as control.

This method represents a viable alternative for screening proteins in selective autophagy. With a single dish of cells, the EGFP signal of DUBs can vary due to the different transfection efficiency between cells. Additionally, the results are based on single cell, which can reflect the DUB effect more accurately compared to averaging the results for several cells in an image. Coordinated with stitching the images, the number of cells under quantification can be easily manipulated. Moreover, the Ub signal can be calculated only on the damaged organelles rather than pooling the Ub signal in the whole cells.



doi:10.6342/NTU201704022

Thus, the strategy was tested first in mitophagy with expressing the known DUB, USP30, as a criteria of the testing. Upon the assay was establishing, some problems were found and solutions were tested. Meanwhile, there were 27 usable DUB constructs in the library, and conditions of screening DUBs in lysophagy and golgiphagy were set. After validation of the assay, we believe that we have designed an innovative solution for screening the DUB in selective autophagy.



doi:10.6342/NTU201704022

# Materials and Methods

## Materials

- 0.5% Trypsin-EDTA (10X) (Thermo Fisher Scientific, 15400-054).
- 1 Kb DNA Ladder (Geneaid, DL006).
- Al (III) phthalocyanine chloride disulfonic acid ($AlPcS_{2a}$), (Frontier Scientific, P40632).
- Albumin, bovine, Fraction V, pH 7, heat-shock fractionated (Affymetrix/USB, J10857).
- Antibiotics
    - Carbenicillin (Disodium) (Gold Biotechnology, C-103-25).
    - Kanamycin Monosulfate, USP Grade (Gold Biotechnology, K-120-25).
    - G-418 Sulfate (Gold Biotechnology, G-418-5).
- Antibodies
    - Anti-DDDDK tag antibody, goat polyclonal (Abcam, ab1257).
    - Anti-Myc tag antibody - ChIP Grade (Abcam, ab9132).
    - Anti-Ubiquitinylated proteins, clone FK2, mouse monoclonal IgG1 (Millipore, 04-263).
    - Donkey Anti-Goat IgG H&L (Alexa Fluor® 405) preadsorbed (Abcam, ab175665).



doi:10.6342/NTU201704022

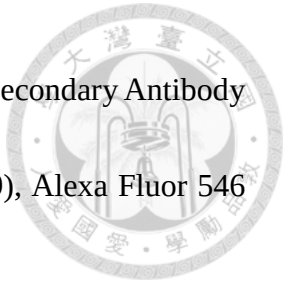

- Goat anti-Mouse IgG (H+L) Highly Cross-Adsorbed Secondary Antibody (Thermo Fisher Scientific), Alexa Fluor 488(A-11029), Alexa Fluor 546 (A-11030).
- Goat anti-Mouse IgG (H+L) Secondary Antibody, Alexa Fluor 405 (Thermo Fisher Scientific, A-31553).
- Goat anti-Rabbit IgG (H+L) Highly Cross-Adsorbed Secondary Antibody, Alexa Fluor 546 (Thermo Fisher Scientific, A-11030).
- Goat anti-Rabbit IgG (H+L) Secondary Antibody, Alexa Fluor 405 (Thermo Fisher Scientific, A-31556).
- LAMP1 (D2D11) XP® Rabbit mAb (Cell Signaling, 9091).

- CCCP (2-[2-(3-Chlorophenyl)hydrazinylyidene]propanedinitrile) (Sigma, C2759)
- Competent cells (Made by our lab, with protocol from (Tu et al., 2005)).
- Dimethyl sulfoxide (DMSO) (Sigma, D2650).
- Dulbecco's Modified Eagle Medium (DMEM) (Thermo Fisher Scientific, 11965-092).
- Fetal Bovine serum (FBS) (Gibco, 26140-079).
- Gel Loading Dye, Purple (6X) (New England BioLabs, B7024S).
- HCS CellMask™ Deep Red stain (Thermo Fisher Scientific, C10046).
- HEPES (N-2-hydroxyethylpiperazine-N-2-ethane sulfonic acid, Gibco, 15630080).



doi:10.6342/NTU201704022

- High-Speed Plasmid Mini Kit (Geneaid, PD300).
- Immersion Oil Type-F (Olympus, Z-81226).
- LB Agar, Miller (Luria-Bertani) (Difco,BD, 244520).
- LB Broth, Miller (Luria-Bertani) (Difco BD, 244620).
- Lipofectamine 2000 (Thermo Fisher Scientific, 11668).
- MitoTracker® Deep Red FM (Thermo Fisher Scientific,).
- NucleoBond® Xtra Midi (MACHEREY-NAGEL, 704010.50).
- Opti-MEM® I Reduced Serum Medium (Thermo Fisher Scientific, 31985-070).
- Paraformaldehyde 16% (formaldehyde) aqueous solution (Electron Microscopy Sciences, 15710).
- Penicillin and streptomycin (P/S) liquid (Thermo Fisher Scientific, 15140-122).
- Phosphate-buffered saline (PBS): 0.137mM NaCl, 2.7mM KCl, 8.0mM $Na_2HPO_4$, 1.76mM $KH_2PO_4$, pH 7.5.
- Phusion Flash High-Fidelity PCR Master Mix (Thermo Fisher Scientific, F548L).
- Phusion High-Fidelity PCR Master Mix with HF Buffer (Thermo Fisher Scientific, F531L).
- Plasmid Maxi Kit (QIAGEN, 12165).
- Plasmid Mini Kit (QIAGEN, 12125).
- Plasmids (Table 1).



doi:10.6342/NTU201704022

- Restriction enzymes (NEB, Table 1).
- Soduim hydroxide (NaOH), Pellet (ACS) (UniReigion Bio-Tech, F0970).
- SYBR® Safe DNA Gel Stain (Thermo Fisher Scientific, S33102).
- T4 DNA ligase (New England BioLabs, M0202S).
- T4 Polynucleotide Kinase (PNK) (New England BioLabs, M0201L).
- Trypan Blue Solution, 0.4% (Thermo Fisher Scientific, 15250061).
- QIAquick Gel Extraction Kit (QIAGEN, 28706).
- Quick Ligation™ Kit (New England BioLabs, M2200S).
- Ultra-Pure Taq PCR Master Mix (Geneaid, UTM200).
- Zinc phthalocyanine (ZnPc) (Sigma-Aldrich, 341169-25G)

## Equipment

- Autofluorescent Plastic Slides (Chroma, 92001).
- Advanced Four-Channel LED Driver (Thorlabs, DC4100).
- BRAND® PARAFILM® M sealing film (Aldrich, BR701605).
- Bright-Line Hemacytometer (Hausser Scientific, 1490).
- Confocal fluorescence microscope (Olympus, FV1000), will be detailed in the following description (Methods-Cellular imaging and analysis).



doi:10.6342/NTU201704022

- Deep Red (660 nm) Collimated LED for Olympus BX & IX, 1200 mA (Thorlabs, M660L3-C1).
- DNA Engine® Peltier Thermal Cycler (BioRad, PTC-0200).
- FACS Aria II cell sorter (BD Biocsiences, in IBMS, Academia Sinica).
- Falcon® 5mL Round Bottom Polystyrene Test Tube, with Cell Strainer Snap Cap, (Corning, 352235)
- Filters (0.22μm) (Sartorius, 16534).
- Glass bottom dishes | 35 mm Dish | No. 1.5 Coverslip (MatTek corporation).
  - 14 mm Glass Diameter | Uncoated (P35G-1.5-14-C).
  - 20 mm Glass Diameter | Uncoated (P35G-1.5-20-C).
- Neon® Transfection System (Thermo Fisher Scientific, MPK5000).
- Syringe (Terumo, SS-01T).
- UVP, BioDoc-It$^{TM}$ Imaging System.



doi:10.6342/NTU201704022

# Methods

## Plasmids

The DUB library was set up by cloning DUB into pEGFP-C1 vector (Fig. 1). All the DUBs were tagged with EGFP at N' terminus. The detailed information of the commercial plasmids was described in Table 1.

## Cloning

The backbone of DUBs were from commercial plasmids, which was listed in Table 1. The restriction enzyme cutting sequences were added at the 5' terminus of primers for replicating the DUB gene by PCR. The conditions of PCR reaction were listed in Table 2. The template segments in PCR products were digested by adding 1 μl DpnI (NEB, R0176L) in 50 μl PCR reaction for ≧4 hr at 37℃. After PCR products were cleanup by Gel Extraction kit, the DUB sequences and EGFP-C1 vector were digested simultaneously by two restriction enzymes (double digestion) at 37℃ overnight (Table 3). Next, the digestion products were purified by cutting bands on agarose gel of DNA electrophoresis. The DUB gene (insert) and EGFP-C1 vector were purified by Gel Extraction kit, and annealed by T4 ligase at 4℃ overnight with volume ratio of insert : vector = 1:1 or 1:3 or 1:5 or 1:7 (Table 3) . By heat shock of E.*coli* DH5α competent cells



doi:10.6342/NTU201704022

at 42℃ for 45 sec., the ligation product was transformed and incubated for 1 hr in LB broth. Later, the E.*coli* was cultured on LB agar plates with kanamycin selection. For further checking on the plasmid sequences, the single colony was picked by 10 μl tip, and directly used as PCR template with a dip in the PCR reaction (Table 2). Simultaneously, the plasmid strain was streaked on a LB plate by the tip and cultured at 37℃ overnight. The PCR checking primers are sequences on EGFP-C1 vector backbone: EGFP-C1-CMV-Forward (GGCACCAAAATCAACGGGAC) and EGFP-C1-MCS-Reverse (GTTTCAGGTTCAGGGGGAGG). After evaluating the size of PCR product by DNA gel electrophoresis, the single colony showed the right DNA size was cultured in LB broth and purified by Miniprep kit. The plasmid showed correct sequences in sequencing results by primers: EGFP-C1-CMV-Forward, EGFP-C1-K126-Forward (GAAGGGCATCGACTTCAAGG) and EGFP-C1-MCS-Reverse, was purified by Midiprep kit and ready for transfection into cells.

For site-directed mutagenesis, the 5' end of primers were added phosphates by T4 PNK at 37℃ for ≧4 hr first, and inactivate the kinase at 65℃ for 20 min (Table 3). The phosphate primers were then used in PCR (Table 2). The rest of the steps are the same as regular cloning that described above.



doi:10.6342/NTU201704022

## Cell culture and seeding

HeLa cells were cultured in DMEM supplemented with 10% FBS and 1% P/S. HeLa cells, which stably expressing EBFP2-Parkin (Yang and Yang, 2011), were selected by G418 (stock 400mg/ml, diluted with 1M HEPES). All cells were maintained at 37 °C with 5% $CO_2$ and exchange fresh DMEM every 2~3 days.

For seeding cells on glass bottom dish, dishes were coated by polylysine under room temperature for 10 min and rinsed by PBS three times. Cells cultured in 10-cm dish were trypsinized and the cells were counted by Hemacytometer. The cells were mixed with 1ml DMEM with $10^5$ cells/ml per glass bottom dish with homogeneous separation by shaking the dish. Finally, cells were maintained at 37 °C with 5% $CO_2$ overnight.

## Transfection

- **By Lipofectamine 2000**

Cells were seeded on glass bottom dish a day before transfection. For transfect plasmid, 0.5~1μg total amount of plasmid DNA was diluted by 50 μl OptiMEM-I in one microtube and 0.5~1 μl Lipofectamine 2000 reagent was diluted into another microtube of 50 μl OptiMEM-I. After placing at room temperature for 5 min, two solutions were mixed by gently pipetting and then placed at room temperature for another 30min.



doi:10.6342/NTU201704022

Subsequently, the transfection mixture was mixed with 100 µl of antibiotic-free DMEM (without P/S) to reach 200 µl of final volume and it was added drop by drop onto the glass coverslip region of the 35-mm glass button dish. After incubation at 37°C for 2 hours, the transfection mixture was replaced by fresh antibiotic-free medium.

- **By electroporation**

The detailed steps were followed by user guide of Neon® Transfection System (page 14~21). 2µg of plasmid DNA (EGFP or EGFP-USP30) were mix with 50 µl mixture of $10^6$ cells and Buffer R, which was operated with 1500V, 10ms for 3 pulses when electroporation.

## Lysophagy assay

First, the cells were transfected with EGFP-DUB, EGFP-C1(as control), pRK5-myc and p3xFLAG-CMV™-7.1 in a ratio of DNA: lipofectamine = 1µg: 0.5µl. The stock of AlPcS2a was prepared by Yu-Hsien Hung (Hung et al., 2013) and was diluted 1000X by antibiotic-free DMEM to final 125nM in cell staining. The dye was added 1ml per dish with seeding cells and incubated at 37°C for 16hr. De-staining was required after staining by replacing the dye with 1ml antibiotic-free DMEM for incubating at least 6 hr at 37°C with 5% $CO_2$. To induce lysophagy, the cells were illuminated by 650nm, 1200mA LED



doi:10.6342/NTU201704022

light for 1~2 min and incubated for 90 min (for Ub recruitment) at 37°C with 5% $CO_2$ after illumination. Finally, the cells were treated by immunofluorescence.

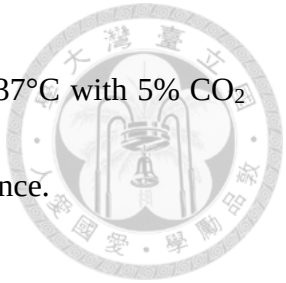

## Mitophagy assay

Mitophagy was induced by CCCP or Mitotracker with illiminaiton (Hsieh et al., 2015; Narendra et al., 2008). For CCCP treatment, the drug was used in 10μM with antibiotic-free DMEM for incubating 2 hr at 37°C with 5% $CO_2$. Mitotracker DeepRed was diluted to final 200nM with antibiotic-free DMEM for incubating 30min at 37°C with 5% $CO_2$. After de-stained by PBS washing for 3 times, the cells were illuminated by 650nm,1200mA LED light for 1 min and incubated for 90 min (for Ub recruitment) at 37°C with 5% $CO_2$ after illumination. Finally, the cells were treated by immunofluorescence.

## Golgiphagy assay

First, the cells were transfected with EGFP-VCPIP1 and mCherry-Golgi7 in a ratio of EGFP-VCPIP1: mCherry-Golgi7: lipofectamine = 600ng: 100ng 0.75μl. The stock of ZnPc (200 μM) was prepared by Hsiang-Yi Chang, and was diluted 1000X by antibiotic-free DMEM to final 200nM in cell staining (Fabris et al., 2001). The dye was added 1ml per dish with seeding cells and incubated at 37°C for 16hr. De-staining was required after



doi:10.6342/NTU201704022

staining by replacing the dye with 1ml antibiotic-free DMEM for incubating at least 3 hr at 37°C with 5% $CO_2$. To induce golgiphagy, the cells were illuminated by 650nm, 1200mA LED light for 2 min and incubated for 90 min (for Ub recruitment) at 37°C with 5% $CO_2$ after illumination. Finally, the cells were treated by immunofluorescence.

## Immunofluorescence

Cells were fixed with 4% paraformaldehyde in PBS (prepared from 16% paraformaldehyde stock) for 10 min. Following permeabilization with 0.25% Triton X-100 in PBS for 10 min, and blocking with 2% BSA in PBS for 30 min, the cells were incubated with primary antibody (1:1000 dilution in 2% BSA-PBS) for 1 hr. Afterwards, Alexa dye conjugated-secondary antibody (1:1000 dilution in 2% BSA-PBS) was added for visualizing primary antibody with incubation for 1 hr. To clearly define cellular region, HCS CellMask™ Deep Red stain was diluted in PBS (1000X dilution from 10mg/ml stock) and applied for 30 min. The cells were finally rinsed in 2ml PBS per dish for further imaging. All the processes were completed at room temperature with PBS washing for three times between each steps.

## Fluorescence-activated cell sorting (FACs)

First, the sorting buffer was prepare by adding 1% FBS and 25mM HEPES in PBS,



doi:10.6342/NTU201704022

and filtered by 0.22 μm filter. The cells ($10^6$ cells/ml were recommended) were trypsinized and re-suspended by 3 ml antibiotic-free DMEM, afterwards with centrifugation for 3min, 1000 xg at room temperature. The supernatant was discarded in replacement of 1 ml sorting buffer with thoroughly re-suspension. Next, the Falcon® 5mL tube with filter on the cap was prepared, and the cell mixture was filtered by pushing the cells gently with pressing the pipette tips directly against the filter. The cap of the tube with cells was sealed by parafilm to prevent contamination, and was put on ice with light avoidance. For collecting the cells from sorting, 3 ml non-antibiotic DMEM was prepared in 15ml centrifugation tube or 200 μl/well in 96 well plates. The cells and the collecting martirals were delivered to the IBMS Flow Cytometry Core (N704) for cells sorting. In this study, the EBFP2-parkin HeLa stable cell line was sorted with near UV laser by FACSAria II cell sorter.

## Cellular imaging and analysis

All Immunofluorescence images were acquired with Olympus IX81 confocal microscopy by a 60X/1.40 ∞/0.17 oil microscope objective (Olympus, PlanApo 60X), and immersion Oil was required for imaging. The microscopy was equipped with an automatic XY stage controller (Applied Scientific Instrumentation, MS-2000), a digital camera (Hamamatsu, C11440-22CU) to obtain 16-bit images, a confocal spinning disk



doi:10.6342/NTU201704022

(Yokogawa, CSU-X1), and controlled by software MetaMorph Hamamatsu. The detailed conditions of laser intensity and emission collecting range were listed in Table 4. ZDC zero-drift autofocus system (Olympus) was used to compensate sample drift in the z direction for real-time image acquisition ("Device/ Focus/ set continuous focus/ start continuous focus" in Metemoroph).

The images were obtained and montaged by "Scan Slides", and processed by "Background and Shading correction" in MetaMorph. Images were converted to 8-bit by using ImageJ software (https://imagej.nih.gov/ij/). Automated quantifications were performed by ScanR Analysis (Olympus). Generation of graphs and statistical analysis were performed by Excel (Microsoft Corporation).

- **Image processing with "Background and Shading correction" and "Scan Slides" montage in MetaMorph**

The background images of camera were obtained with the laser intensity = 0, while the shading images were acquired with a single color slides when laser intensity =100 (Maximum value) and subtract background by the "Substract background" function in "Background and Shading correction" (Fig 2a). The correction formula of "Background and Shading correction" in MetaMorph was

$$\left(\frac{input\ image-background}{shading\ image-backgrund}\right) \times scaling\ factor.$$



doi:10.6342/NTU201704022

The scaling factor was set as 0.01. The correction was applied on corresponding laser wavelengths. After correction, the images were montaged by "Scan Slides" apps in MetaMorph with 10% coverage of each image.

- **Image analysis by "ScanR Analysis"**

Under the assumption of this study, the images were required to be analyzed by cellular level. As a result, the ScanR Analysis software was used since it could define the cell region as "Main object", which could analyze other signals from different channels on specific main objects. The analysis assay was established by Matthias Rommeswinkel (Application Specialist in Olympus Soft Imaging Solutions GmbH).

First, the images files need to be renamed by the rules "--W00001--P00001--Z00000--T00000--'channel name'" in order to be recognized by ScanR Analysis. The channel name was corresponded to the laser wavelength used when imaging, and the number "P00001" in the file name increased as "P00002" with the second batch of images without changing other numbers in the file names. In the study, channel name "BFP" is for 405 nm laser, "EGFP" for 488 nm laser, "TRITC" for 561 nm laser, and "DEEPRED" for 640 nm laser excitation. For example, the naming of the second batch of images should be "--W00001--P00002--Z00000--T00000--BFP", "--W00001--P00002--Z00000--T00000--EGFP", "--W00001--P00002--Z00000--T00000--TRITC", "--W00001--



doi:10.6342/NTU201704022

P00002--Z00000--T00000--DEEPRED" respectively for individual images. After renaming, the images were converted to 8-bit by ImageJ (select *Process*→*Batch*→ *Macro*→ run("8-bit");).

Secondly, the images needed to be loaded in the form of ScanR-sepecific type of files. The detail steps for converting the files were listed in Table 5.

Thirdly, settings of the assay were different between each results. The channels need to be processed by the function in "Virtual Channel", such as background correction, smoothing, and simple math for co-localization (Fig 3c~3g, Table 5). The BFP and TRITC channels were processed by "Background correction" (BGC-BFP and BGC-TRITC), and "Smoothing" was applied in EGFP channels. In defining the cells edges, 10 folds of DEEPRED signal was added in "Simple math", and "Smoothing (Median)" was utilized for decreasing the noises form strong signal of nucleuses. For defining the co-localization of BFP and TRITC channels, steps from ❶~❽ were yielded under "Simple math". Because of the limitation settings in the "Simple math" in ScanR, only three channels could be in one equation. Steps ❶~❹ were for creating two same channels by adding all 4 channels together. In step ❺, two identical channels were divided to gain a new channel, named "white_01", with homogeneous signal (intensity=1). To obtain an image with consistent intensity, steps ❻ and ❼ multiplied intensity of "white_01" to 1000 folds, to serve as a denominator in step ❽, which generated the determining channel



doi:10.6342/NTU201704022

for co-localization by multiply intensity of “BGC_BFP” and “BGC-TRITC” channels (Fig. 3c~3g). All the ROI (regions of interest) were selected by setting threshold of signal intensity, which can be manually adjusted (Fig. 3h, 3i).

Next, the “parameters”, such as area, spots count, total intensity and mean intensity, can be selected for analyzing signals in color channel on the objects (Fig. 3j). As a result, in single cell analysis, the signal was detected only on the main objects, that is, inside the single cell area. The “Derived parameters” settings can calculate the results by the function of sum, standard deviation and mean (Fig. 3k).

Lastly, after all the settings were finished, the images could be analyzed (select *Analysis→Run*). The time required for running the program depends on the size of the images, usually 30 to 60 min by the CPU “Intel Core i7-3770K @ 3.50GHz” with 24.0 GB RAM. The data can be exported as .txt files (select *Analysis→Export Table*), which can be loaded and analysis directly by Microsoft Excel.

## Statistics

Raw data from ScanR were sorted to groups and analysis value for mean ± SEM. No raw data were excluded from the analysis. To obtain the correlation between mean intensity of EGFP and Ub/ organelle marker co-localization area per cell, Spearmen’s correlation coefficient ($r_s$) were used and analyzed P-value with one-tailed Student’s t-



doi:10.6342/NTU201704022

test ($t = r_s \times \sqrt{\frac{n-2}{1-{r_s}^2}}$). Pearson's correlation coefficient was used in Fig. 4a~4c .Imaging fields were randomly chosen while imaging. Microsoft Excel was used for the statistics.



doi:10.6342/NTU201704022

# Results

## Shading correction is required for image processing.

As the shading images showed, the intensity decreased from the middle of the image, resulting a lower intensity in four corners (Fig 2a). Because the images were stitched before analysis, the shades in the corner would be a problem for the readout signals. As a result, the “Background and Shading correction” in MetaMorph was a suitable tool to adjust the shades. The shadow of the montaged edge was clearly seen in images without correction (Fig. 2b), resulting an incomplete cell area dictation. As the yellow box showed, the cells with shades were undetectable under the threshold due to lower signal intensity (Fig. 2d, top). However, the cells showed smooth signal after shading correction (Fig. 2c), which in aid of reducing the inadequate cell shape detection (Fig. 2d, bottom). Therefore, shading correction is necessary for image processing before analysis.

## ScanR assay testing by expressing EGFP-USP30 in mitophagy

The ScanR assay was tested by a cropped image from expressing EGFP-USP30 in HeLa cells, and mitophagy was induced by CCCP (Fig. 3a). The Anti-Ub signal was from Goat anti-Mouse IgG Secondary Antibody, Alexa Fluor 546. By eyesight, the EBFP2-Parkin was co-localized with Anti-Ub. The intensity of EGFP-USP30 was different



doi:10.6342/NTU201704022

between cells due to the distinct transfection efficiency to each cells, and the Cellmask channel showed the shape and edge of each cell. For clearly identifying the puncta, the magnified images for EBFP2-Parkin and Anti-Ub demonstrated clear co-localization, which represented mitophagy (Fig.3b).

After “background correction” was applied to BFP and TRITC channels, the Anti-Ub and EBFP2-Parkin signals became clearer, and the noises, which shows the cell shapes, were disappeared (Fig. 3c, 3d). In order to decrease the signal differences, smoothing was applied to average the signal (Fig.3e). In Fig.3f and 3g showed “Simple math” panels, which were set respectively for deciding cell area and co-localization puncta area in the later steps. By setting the thresholds for selecting the ROI in individual channels, the cell regions were defined (Fig.3h). Not all the cells were selected under the threshold due to the uneven intensity of cells; for example, the signal intensity in nucleolus was higher than that of cytosol. That is, the threshold cannot be perfectly manipulated for selecting all the cells with the completed cell shape. Accordingly, despite of losing some cells, the threshold should be set for selecting the whole cell area in single cell. In testing the assay, the threshold for main objects was set at 2570, which was ideal for the balance for cell shape integrity and cell number (objects found). For setting the intensity of Smoothing_EGFP channel, low value of threshold was optimal for selecting large area of ROI in case of counting all the cells, because the EGFP intensity would be only measured



doi:10.6342/NTU201704022

on main objects. Compared with the original images in Fig.3b, the puncta analysis in Fig. 3i showed similar pattern. For selecting co-localization channel, the Merge image in Fig. 3b was the criteria, and the puncta was carefully defined for preventing misestimating. The parameter and derived parameter were set for required measurement in the assay (Fig.3j, 3k).

## The ScanR analysis assay is applicable on single cell measurement

To justify whether the ScanR assay could reflect the image results, the statistical measurement was applied. The three parameters, Parkin area per cell, Ub area per cell and Ub-Parkin co-localization area per cell were analyzed in inetercomparison, which was expected to show positive linear correlation (Fig. 4a~4c). The Pearson correlation coefficient showed positive correlation of the inetercomparison of the three parameters, which indicated that the analysis was match with the image result, showing strong co-localization of Parkin and Ub signals.

Underlying the hypothesis of the study, the ubiquitination of damaged mitochondria would be suppressed by the overexpression of EGFP-USP30. This phenomenon was shown in Fig. 2b, which the cells with high level of EGFP-USP30 expression showed less



doi:10.6342/NTU201704022

Parkin and UB recruitment. By the Spearman correlation, the mean intensity of EGFP-USP30 and Ub-Parkin co-localization area per cell were negatively correlated with significance (Fig. 4d). To decrease the impact of single cell variation, sorting cells in groups were applied for showing the correlation more clearly. The sorting results showed negative correlation of the mean intensity of EGFP-USP30 and Ub-Parkin co-localization area per cell (Fig. 4e). To sum up, the ScanR assay can reflect the image results for providing the systematic screening tool in this study.

## The increase of cell number sorting stable cell line by FACs were suggested when utilizing the ScanR analysis assay.

With further checking the analysis assay, it was applied in mitophagy with increased cell number. EBFP2-Parkin were homogeneously distributed in stable cells under normal condition (Fig. 5a). The HeLa cells were overexpressed EGFP vector as a control experiment to mimic the transfection environment to the cells, which compared with the group of overexpressing EGFP-USP30. In the image form a cropped section of the original large images (Fig. 5b), the EGFP signal showed no preference in Parkin and Ub translocation to damaged mitochondria. However, the statistical results showed negative correlation between mean intensity of EGFP and Ub-Parkin co-localization area per cell,



doi:10.6342/NTU201704022

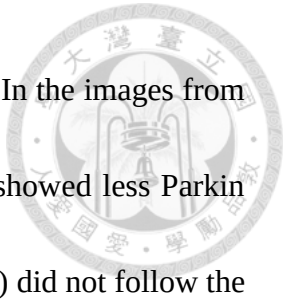

and lack of significance in the correlation (P-value > 0.05) (Fig. 5d). In the images from expressing EGFP-USP30, cells with higher EGFP expression level showed less Parkin and Ub translocation, but some cells (where the white arrows pointed) did not follow the assumption (Fig 5c). From the statistical result of EGFP-USP30 group, the correlation of mean intensity of EGFP-USP30 and Ub-Parkin co-localization area per cell was similar with that of EGFP group (Fig. 5e). In the previous assay testing results, the ScanR assay showed nice performance in image data analysis. Nonetheless, with increased cell number, the results were not fit to our hypothesis. As we can see in the cropped images, some cells showed no Parkin and Ub signals and certainly no Parkin and UB translocation. As a result, we next tried to sort the cells by FACs in IBMS to gain stable cells with higher EBFP2-Parkin expression. The cells had sorted twice, one was selected for top 24.5% cells with high EBFP intensity, and one was further sorted for the top 1.3% cells (Fig. 6a, 6b). We first defined when the Parkin area in a cell was lower than 200 pixels, the cells were no Parkin translocation. Originally, 47.62% cells showed no Parkin translocation, and transferred to 26.84% cells without Parkin recruitment after the first sorting (Fig. 6c). Later, the cells were sorted for the second time, and showed 17.24% of no Parkin translocation, which the cells was used in the following experiments. With comparison of the cells with Parkin translocation under mitophagy, sorting could be benefit for the stable cells to express EBFP2-Parkin, and in aid of inducing mitophagy.



doi:10.6342/NTU201704022

## The ScanR assay was tested by illuminated Mitotracker induced mitophagy.

After sorting, the ScanR assay was tested by another way to induce mitophagy: illuminated Mitotracker. Similar with the experimental processes except the mitophagy induced part in Fig. 5, EGFP or EGFP-USP30 were transfected by lipofectamine. Like the results showed in Fig. 5b, the EGFP expression level seemed not effecting Parkin or Ub translocation (Fig. 7a). Nonetheless, the statistical results showed that mean intensity of EGFP and Ub-Parkin co-localization area per cell were native correlated with no significance (P-value > 0.05) (Fig. 7c). In the group of EGFP-USP30, the images showed that cells with EGFP-USP30 expressing can suppressed Parkin translocation and Ub resuiment (Fig.7d). However, the statistical result showed no significant negative corelaion between mean intensity of EGFP-USP30 and Ub-Parkin co-localization area per cell. Therefore, the assay remained some problems that need to be handled.

## Test the ScanR assay by changing the transfection methods

In the previous results, the EGFP group was served as a control group that the correlation between mean intensity of EGFP and Ub-Parkin co-localization area per cell should be weaker than that in EGFP-USP30. While the results in inducing mitophagy by CCCP or



doi:10.6342/NTU201704022

illuminating Mitotracker were not fit to the assumption or the correlation was no statistical significance. Studies showed that lipofectamine 2000 had cytotoxicity and lower transfection efficiency (Chernousova and Epple, 2017; Maurisse et al., 2010); therefore, we tried to change the transfection methods to electroporation, which was based on physical transfection to increase permeability of plasma membrane to molecules (Colosimo et al., 2000). In both methods to induce mitophagy, the control groups showed negative correlation between mean intensity of EGFP and Ub-Parkin co-localization area per cell (Fig. 8c, 8g). In the results with expressing EGFP-USP30, the group of CCCP induced mitophagy indicated a negative correlation, but not fit with our assumption, which expected the USP30 could significantly inhibit the Ub signal (Fig. 8h). On the other hand, compared with the control group, the results of illuminated Mitotracker induced mitophagy with expressing EGFP-USP30 demonstrated a significant negative correlation between mean intensity of EGFP and Ub-Parkin co-localization area per cell, which was correspond to the hypothesis (Fig. 8d). To sum up, the transfection methods and the ways to induce mitophagy could be factors to impact the effect of USP30 to Ub signals.

## Test the ScanR assay by different fixation conditions.

In the previous results, the Cellmask channel showed stronger intensity in nucleus than that in cytosol. Meanwhile, the structure of cytoskeleton was clear by the Cellmask stain, which may impact the segmentation quality by ScanR. In order to improve the cells



doi:10.6342/NTU201704022

segmentation in ScanR, the various conditions of PFA concentration (2% or 4% PFA), fixation time (5, 10, 20 min) and temperature (4℃, RT, 37℃) were the factors for searching the best condition for fixation. The Fig. 9a, 9b, 9c, 9d, 9f, 9g, 9h, 9i showed apparent cytoskeleton structure, and Fig. 9j showed stronger signal in the cellular edge and nucleus. The cytoskeleton and bright nucleus could be a limitation in defining cell edges (Fig. 9l). Further, Fig. 9e and 9k showed comparatively homogeneous Cellmask signal, which was in aid of the cell segmentation in ScanR (Fig. 9m). Overall, homogeneous Cellmask signal in cells was an important factor when applied to ScanR, and 4% PFA for 20min treatment under 37℃ may be the suitable condition for fixation.

## The preceding work for applying screening assay

Despite of the results of assay testing was not perfect, the works for screening the DUBs in selective autophagy were simultaneously prepared.

### The progress of setting up the DUB library

It was reported that there were a hundred DUB encoded form human genome (Reyes-Turcu et al., 2009). To establish the screening priority, the DUBs on the candidate list, which was from the mass spectrometry data of lysosome related proteins form Yuan-Ping Chu, were the references for priority (The list was not shown). Meanwhile, the



doi:10.6342/NTU201704022

cellular localization of the DUBs was also a criteria for screening. The DUBs localization were reported in some researches (Clague et al., 2012; Urbé et al., 2012); such as the DUBs at endosomes maybe related to lysosomes.

The EGFP-DUB library was set by cloning the plasmids with DUB sequences into EGFP-C1 vector (Table 1). So far, 20 EGFP-DUBs had been cloned, and 1 EGFP-DUB and 6 DUBs with Flag tag were commercial.

## The conditions in damaging lysosomes

For searching the DUB candidates, the lysophagy should be globally induced in the cells. As a result, determining the suitable conditions to fully damaged lysosomes was important. The lysophagy assay was established (Chu et al., 2017), but the illumination time of 650 nm LED light to induce lysophagy was different in each experimental condition. Illumination time from 0 to 5 min was tested with overexpressing EGFP by lipofectamine to mimic DUB expressing status, and served Lamp1 as a lysosome marker (Fig. 10a). The cells morphology became abnormal since 3min of illumination, and the cell number in each time point reflected the cell viability. Through the statistical results, illuminating for 3 min was detected for highest Ub-Lamp1 co-localization area per cell (Fig. 10b). However, the cell number was relatively low in 3-min group, which means the cell viability may be low under the condition. Therefore, illuminated for 1 min was the



doi:10.6342/NTU201704022

best condition with considering the Ub recruitment rate to lysosomes and cell viability. The correlation between mean intensity of EGFP and Ub-Lamp1 co-localization area per cell was negative but showed no statistical significance, which was similar to the results form control group in mitophagy with transfecting EGFP by lipofectamine (Fig. 10c). To ensure the ratio between damaged and total lysosomes in cells, the Ub-Lamp1 co-localization area per cell were divided by total Lamp1 area per cell (Fig. 10d). Most of the cells reacted a 15-20% damaged lysosomes and also showed a negative correlation between ratio of Ub recriutment to Lamp1 per cell and EGFP expression level.

## The DUBs tested in lysophagy: OTUD6A and USP10 may be the candidates in reversing lysophagy

So far we have tested 9 DUBs, including OTULIN, OTUD6A, UCHL1, UCHL3, USP5, USP10, USP30, USP50 and YOD1, in screening the candidates for opposing lysophagy. These DUBs showed various types of cellular localization; OTULIN and YOD1 were homogeneously distributed in cells; UCHL1, UCHL3 and USP5 were mainly in nucleus and partly in cytosol; USP10 was mainly in the cytosol; OTUD6A, USP30, USP50 were spread in the cells but formed puncta near the location of Ub (Fig. 11a,11b). In the statistical analysis, only USP10 and OTUD6A showed significant negative



doi:10.6342/NTU201704022

correlation between mean intensity of EGFP-DUB and Ub-Parkin co-localization area per cell (Fig. 11c), which may be the candidates for inhibiting lysophagy.

## The Flag-tagged and myc-tagged vectors showed no significant impact on Ub recruitment to damaged lysosomes.

Since the previous results showed that EGFP vector may lead to a negative correlation between Ub-Parkin or Ub-Lamp1 and EGFP expression level, different tags were tested for confirming the screening assay. Hela cells were induced lysophagy by illuminating for 1 min, followed the previous description of the essay (Fig. 10). The signal of Flag vector was homogeneously distributed in the cells (Fig. 12a), while myc signal was mainly in the nucleus (Fig. 12d). The correlation between Lamp1-Ub co-localized area per cell and flag expression level was positive, which was different form the result in EGFP expression (Fig. 10c). On the other hand, it reacted a 20-40% damaged lysosomes per cells, and showed a negative correlation between ratio of Ub recriutment to Lamp1 per cell and Flag expression level without significance. As shown in Fig. 12e and f, the correlation between Lamp1-Ub co-localized area per cell and myc expression level was negative, but ratio of Ub recriutment to Lamp1 per cell and Flag expression level were positively correlated, which also reacted a 20-40% damaged lysosomes per cells. As a



doi:10.6342/NTU201704022

result, the Flag and myc tag signal showed no significant impact on lysophgy, which may also be alternative cloning vectors for establishing DUB library. Furthermore, the impact of expressing EGFP vector in organellophagy required further experiment to confirm.

## The DUB tested in Golgiphagy: VCPIP1 may not be the DUB for opposing Golgiphagy.

In the previous report indicated that VCPIP1, a DUB, could regulate the Golgi membrane dynamics during mitosis (Adler and Parmryd, 2010). As a result, we were curious about whether VCPIP1 could be the DUB that reverse Golgiphagy. By simultaneously transfecting mCherry-Golgi7 as the Golgi marker and EGFP-VCPIP1, Golgiphagy was induced by illuminating ZnPc-stained cells with 650nm LED lights for 2 min. The Ub, VCPIP1 were localized on Golgi under Golgiphagy (Fig. 13a). The statistical results demonstrated that mean intensity of EGFP-VCPIP1 and Ub-Golgi7 co-localization area per cell were positively correlated (Fig. 13b). Therefore, VCPIP1 may not be the candidate for reversing Golgiphagy.



doi:10.6342/NTU201704022

# Discussion

## The key points in ScanR analysis assay

The quality in defining the main objects is decisive in ScanR analysis assay. Without ideal cell area selection, the signals of cellular proteins may distribute out of the defined cell area, which can lead to ignoring the signals. In this study, we chose Cellmask stain for defining the cell area, but higher signals was shown in the nucleus, which increased the possibility of misestimate the cell area. To overcome this problem, the threshold was adjust to lower value for completely selecting the actual cell area. On the other hand, low threshold led to less cell number, since some cells could not be segmented well and excluded by size settings. The cell segmentation quality can be controlled by the cell seeding density, which is affected by the cell number when seeding and the even distribution of the cells on the dish. Overall, the completeness of cell area were prior than cell number when analyzing, which sample number can be compensate by obtaining more images for analysis.

## The negative correlation of EGFP groups

We assumed that EGFP expression would not affect Ub recruitment to damaged organelles, thus showing no relation in statistical results. However, in the results of



doi:10.6342/NTU201704022

different treatment in mitophagy and lysophagy, the EGFP groups all showed a negative correlation between mean intensity of EGFP and Ub-Parkin (or Lamp1) co-localization area per cell (Fig 5d, 7c, 8c, 8g, 10c,), which was not correspond to our hypothesis. The possible explanation of the phenomenon is that the transfection reagent, Lipofectamine 2000, and drug for inducing mitophagy, CCCP, can both increase cell viability (Adler and Parmryd, 2010; Hunt et al., 2010; Yang et al., 2001), causing the attached cells to swell (Ziegler and Groscurth, 2004), and lead to a misestimated mitochondria number. The round morphology of attached cells is a sign of abnormality and cell death (Ziegler and Groscurth, 2004), which may impact the mitochondria morphology to be fragmented and unable to detect on imaging plane (Karbowski and Youle, 2003). Therefore, the higher the EGFP expression level in cells, the more mitochondria are neglected, leading a decrease in Ub and Parkin detection. For lysophagy, the EGFP group showed a similar results of that in mitophagy (Fig. 10c). Previous study showed that lysosome became smaller and more abundant when triggered cell death (Bottone et al., 2013), which can result in the miss of lysosome detection and lowering the Ub/Lamp1 co-localization area. To reduce the transfection side effect, virus infection for DUB overexpression is a possible solution since the DUBs form Wade Harper's lab were originally for retroviral expression system (Sowa et al., 2009).

On the other hand, the side effect of EGFP fusion proteins can be another reason for



doi:10.6342/NTU201704022

the decreased Ub recruitment level in this study. GFP was reported for inducing apoptosis in cell lines including NIH/3T3, Huh-7 and HepG2 (Liu et al., 1999). Another report showed that EGFP and EGFP- tagged proteins can suppress polyubiquitination in NF-kB signaling (Baens et al., 2006). To overcome this issue, changing the reporter marker, such as GFP analog, CFP and YFP, which were demonstrated to have lower cytotoxicity (Taghizadeh and Sherley, 2008), could be the substitution of EGFP. Likewise, linking DUBs with smaller tags, such as Flag and HA tag, which can be detected by immunofluorescence, is another potential solution for EGFP side effects (Fig. 12).

## Optional ways for screening

Apart from overexpression, knockdown of DUBs for further confirmation of candidates is also practical. In the opposite effect of overexpression, we expected that the Ub recruitment on damaged organelles will be increased under DUB inhibition compared to wild type conditions.

Other than the strategy in the study, screening DUB candidates through Ub signals, LC3, one of the autophagic markers, can be another standard for screening the potential DUBs. In autophagy, the pro-LC3 is cleaved by protease Atg4 to LC3-I (Satoo et al., 2009), and is conjugated to phosphatidylethanolamine (PE) by Ub-like conjugation system, Atg7 (E1-like enzyme) and Atg3 (E2-like enzyme), to form the LC3-PE



doi:10.6342/NTU201704022

conjugate (LC3-II) (Kabeya et al., 2000; Tanida et al., 2004). LC3-II will associate on the autophagosomal membrane to facilitate membrane curvature and cargo recognition (Nath et al., 2014). Therefore, for DUBs in regulating organellophagy, the Ub is the upstream signals, while LC3 is downstream. The benefit in screening DUBs by Ub signals is to directly evaluate the cleavage effect of DUBs to Ub. Besides, the strategy of screening DUBs by LC3 signals can ensure that the occurrence of autophagy, but not knowing the DUB impacts general or selective autophagy. Accordingly, for confirming the DUB candidates, screening DUBs by LC3 signals can be an alternative way to coordinate the Ub screening assay.



doi:10.6342/NTU201704022

# Figures and Tables

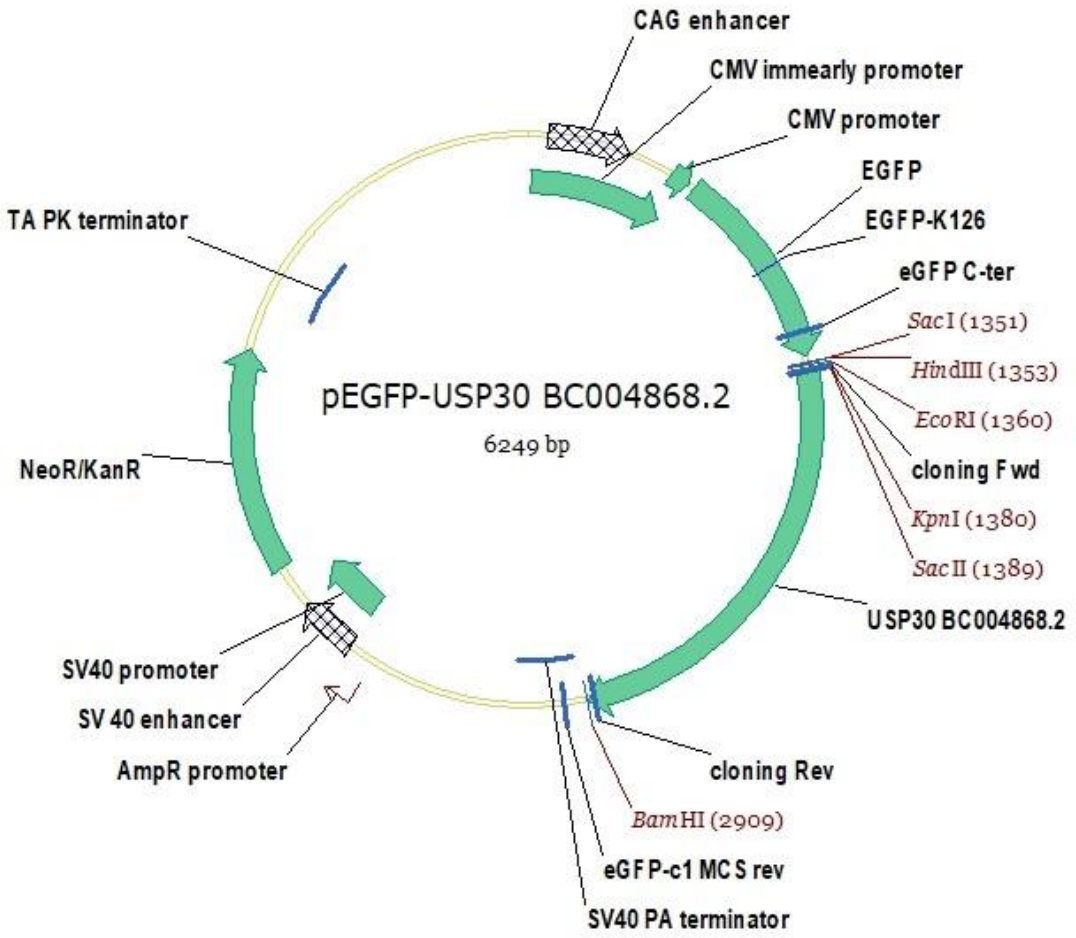


**Figure 1. The map of EGFP-DUB plasmids (EGFP-USP30 as example).**

The EGFP was linked to N' terminal of DUB, which was cloned by cut and paste with restriction enzymes and ligation.



doi:10.6342/NTU201704022

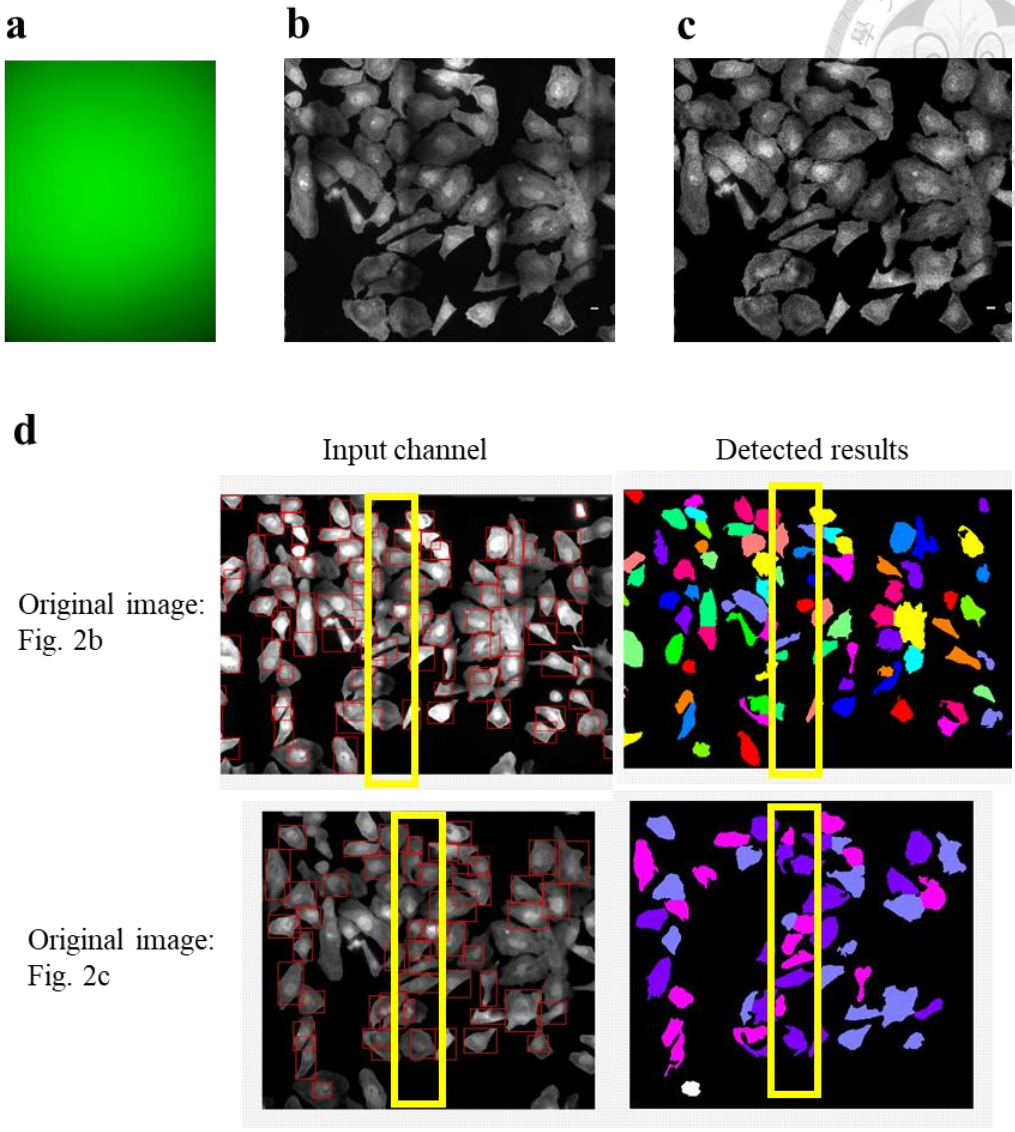


**Figure 2. Shading correction is required for image processing.**

(a) The shading image from 488nm laser.

(b) The Cellmask channel from laser 640nm without shading correction. Scale bars, 10μm.

(c) The Cellmask channel from laser 640nm with shading correction. Scale bars, 10μm.

(d) The images without shading correction were analyzed by ScanR in main objects detection, which showed clear edge of shades.



doi:10.6342/NTU201704022

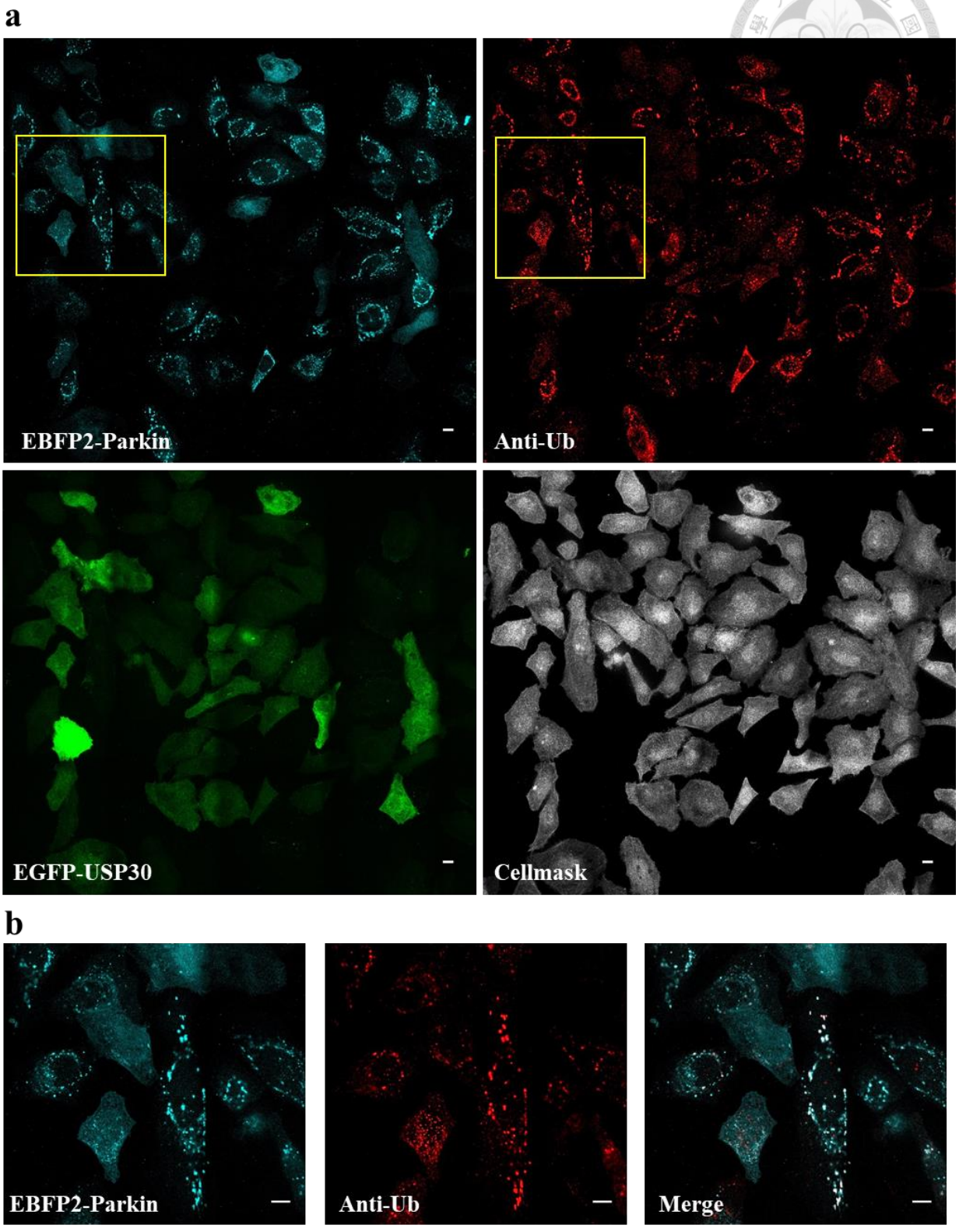




doi:10.6342/NTU201704022

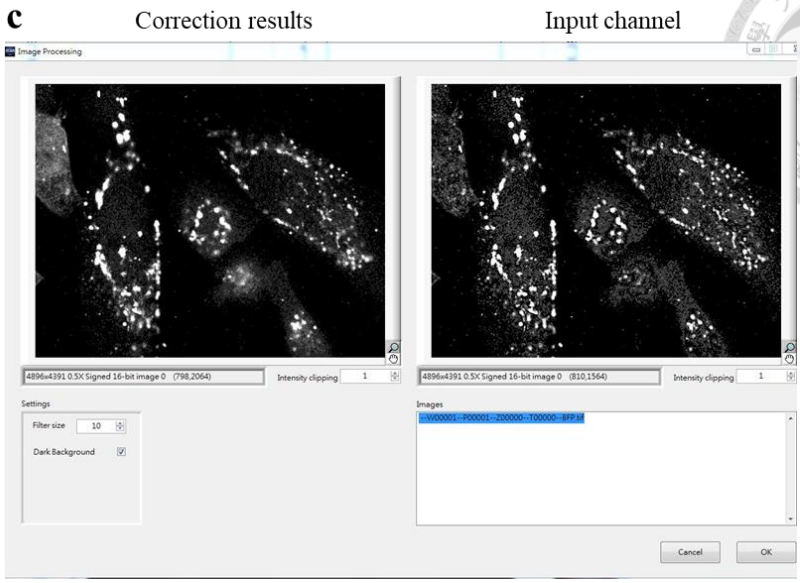


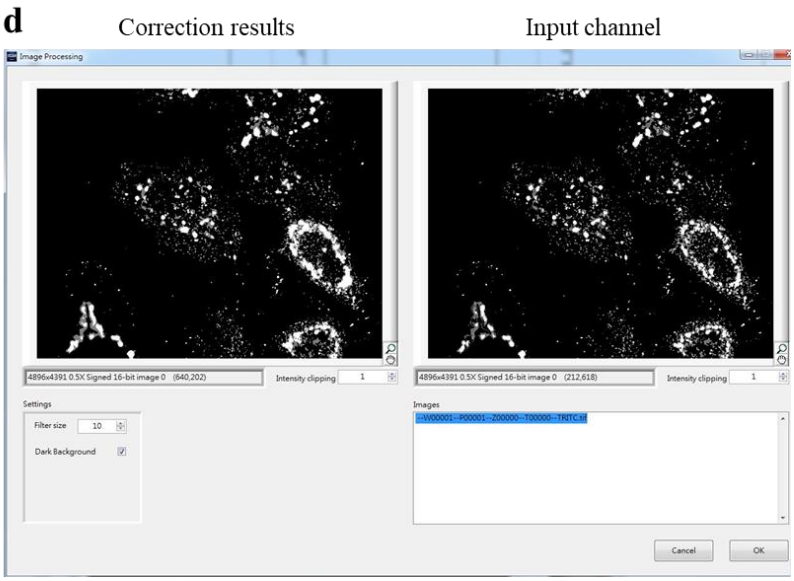


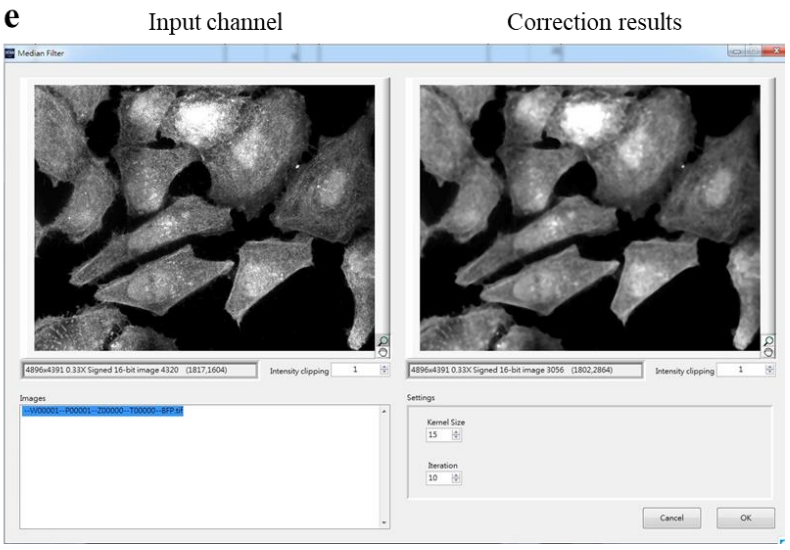




doi:10.6342/NTU201704022

**f**

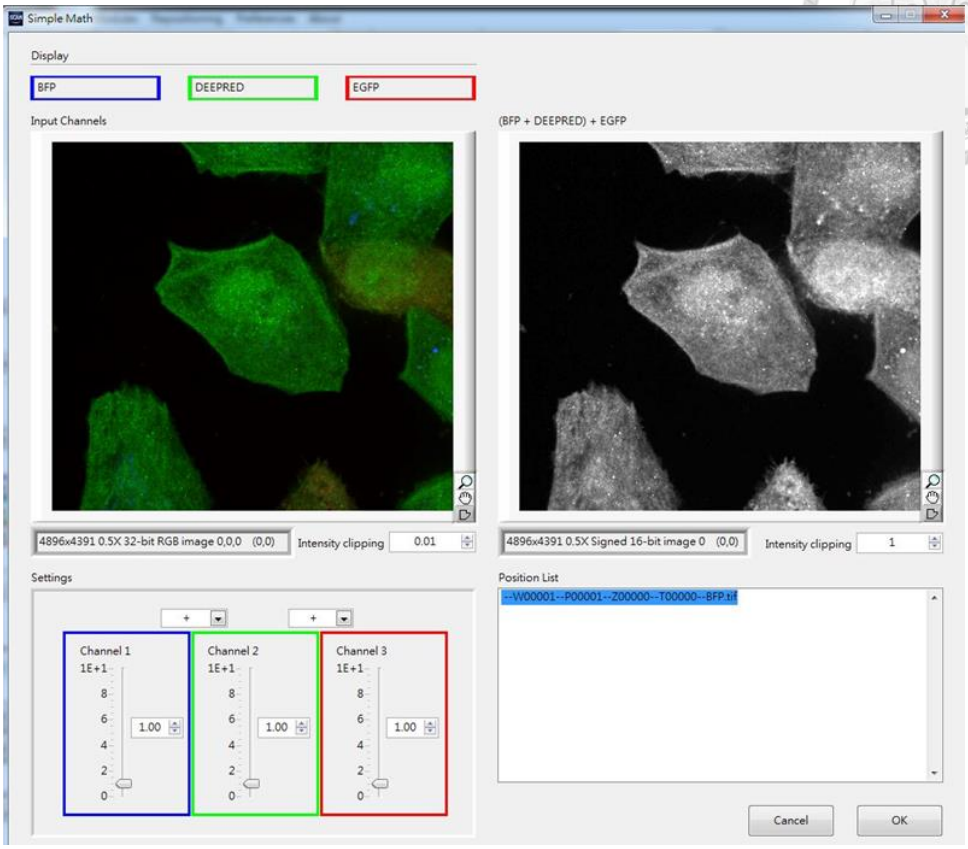


**g**

Input channel Correction results

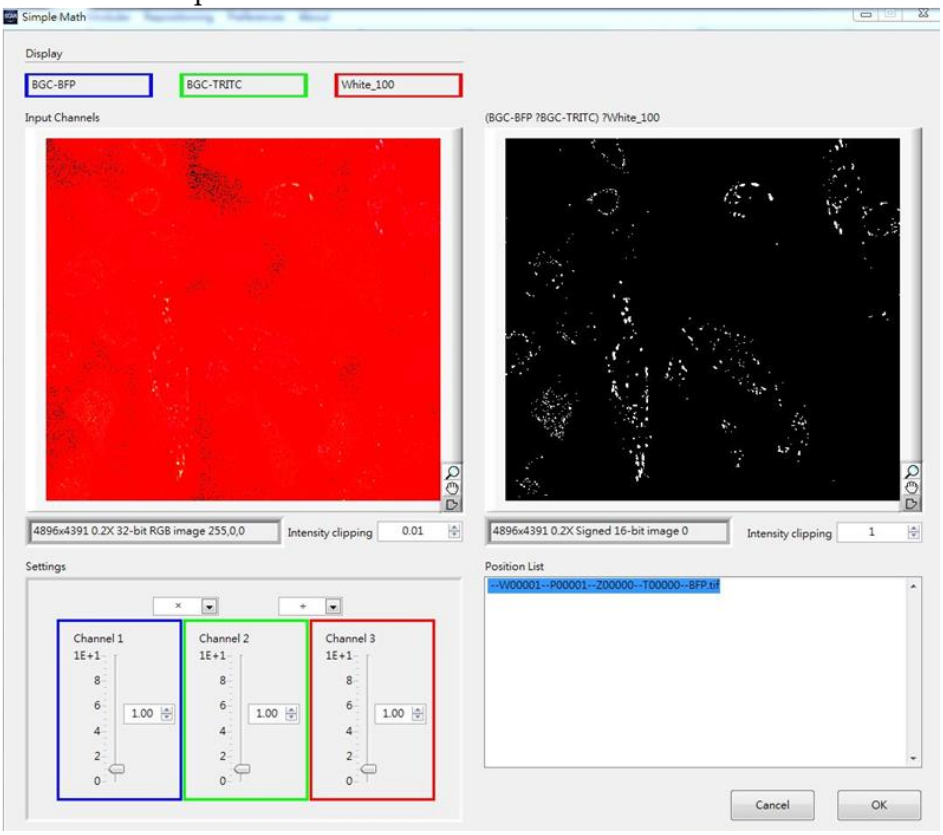




doi:10.6342/NTU201704022

**h**

Input channel

Detected results

All_madian channel

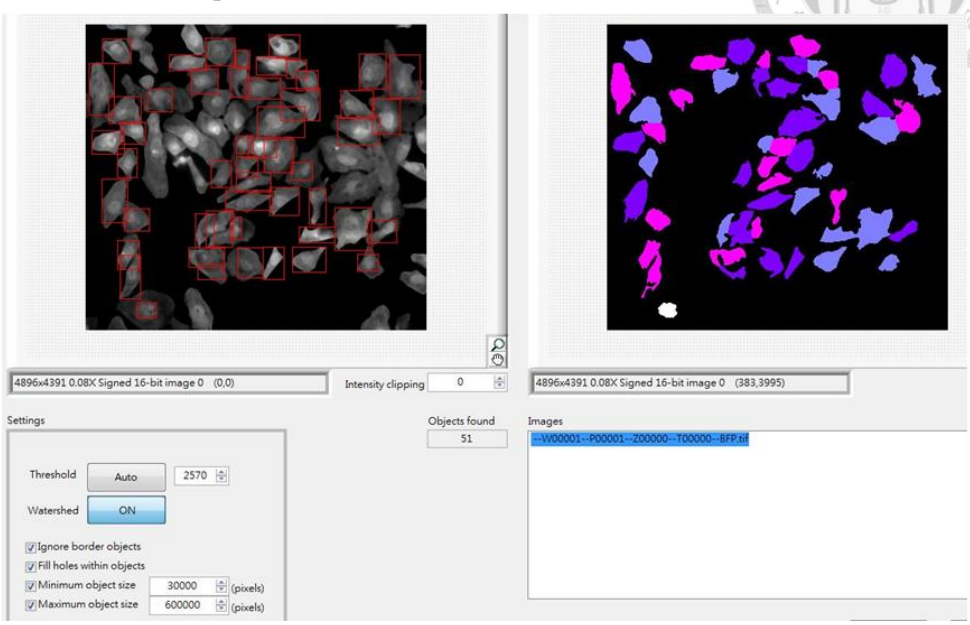


Threshold=2570, Watershed on, Ignore border objects on, Fill holes within objects, Minimum object size=30000 pixels, Maximum object size=600000 pixels

EGFP_ smootning channel

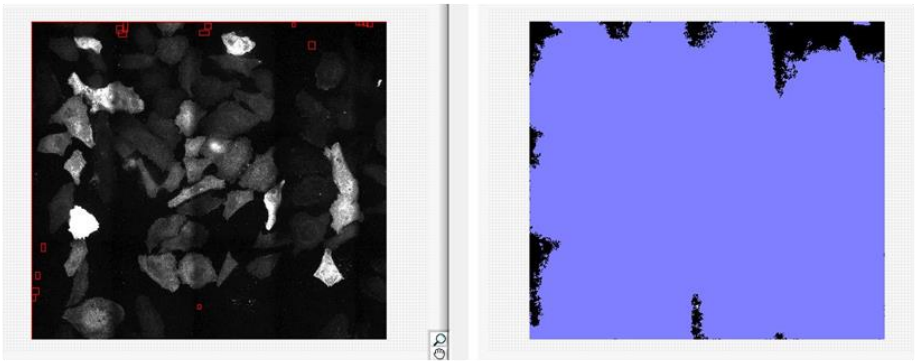

Threshold=16, Watershed on, Fill holes within objects, Minimun object size=1000 pixels



doi:10.6342/NTU201704022

**i**

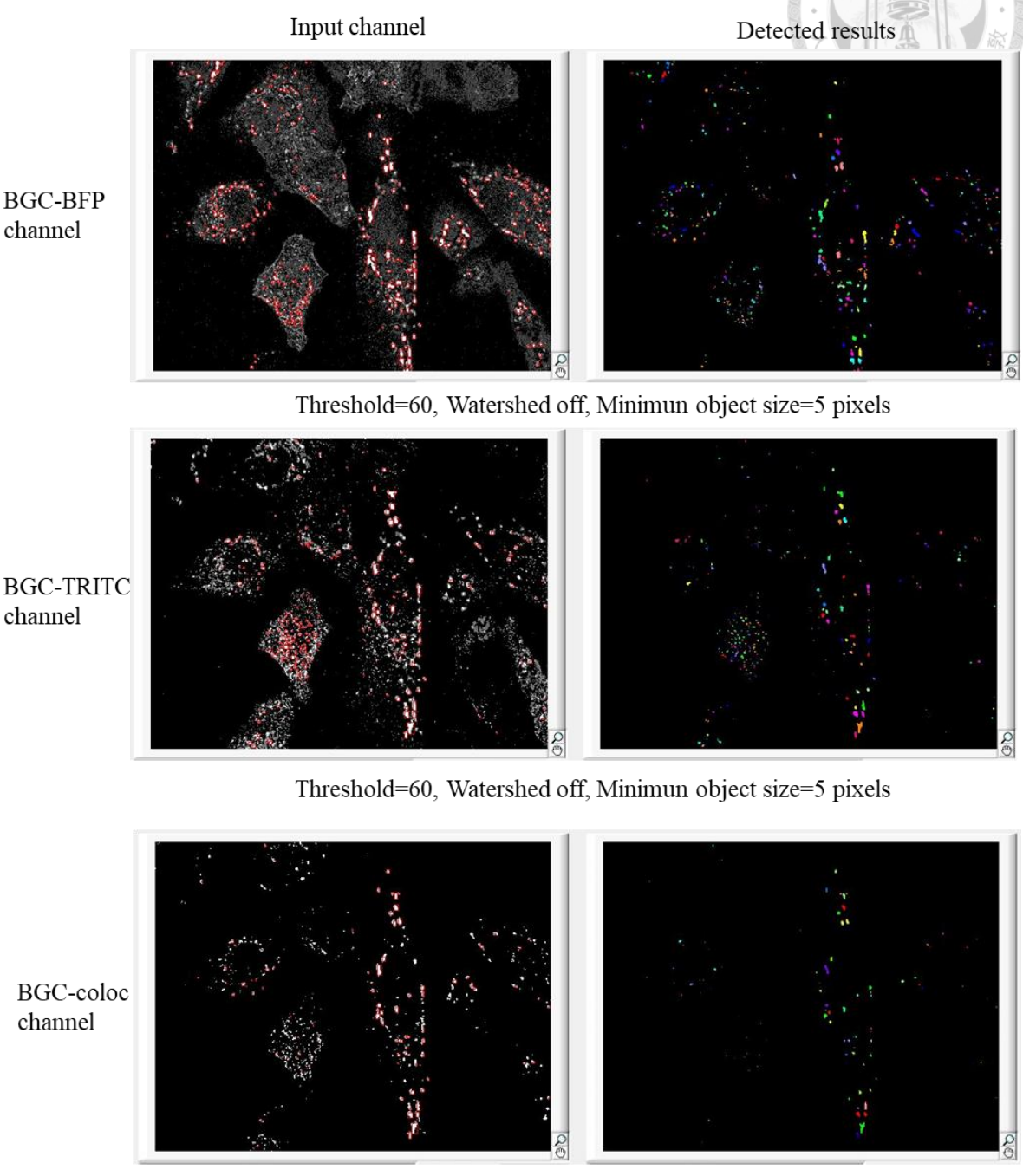




doi:10.6342/NTU201704022

**j**

Assay Settings

Main Object | Sub-objects | Parameters | Derived Parameters | Image Processing | Virtual Channels | Image Export

Parameters

| ID | Measurement | Channel | Object |
|---|---|---|---|
| p1 | Area | | Main |
| p2 | Area | | Blue-Spots |
| p3 | Area | | Red-Spots |
| p4 | Area | | Coloc |
| p5 | Blue-Spots Counts | | Main |
| p6 | Red-Spots Counts | | Main |
| p7 | Coloc Counts | | Main |
| p8 | Total Intensity | BGC-BFP | Main |
| p9 | Mean Intensity | BGC-BFP | Main |
| p10 | Total Intensity | BGC-TRITC | Main |
| p11 | Mean Intensity | BGC-TRITC | Main |
| p12 | Total Intensity | BGC-Coloc | Main |
| p13 | Mean Intensity | BGC-Coloc | Main |
| p14 | Total Intensity | BGC-BFP | Blue-Spots |
| p15 | Mean Intensity | BGC-BFP | Blue-Spots |
| p16 | Total Intensity | BGC-TRITC | Blue-Spots |
| p17 | Mean Intensity | BGC-TRITC | Blue-Spots |
| p18 | Total Intensity | BGC-Coloc | Blue-Spots |
| p19 | Mean Intensity | BGC-Coloc | Blue-Spots |
| p20 | Total Intensity | BGC-BFP | Red-Spots |
| p21 | Mean Intensity | BGC-BFP | Red-Spots |
| p22 | Total Intensity | BGC-TRITC | Red-Spots |
| p23 | Mean Intensity | BGC-TRITC | Red-Spots |
| p24 | Total Intensity | BGC-Coloc | Red-Spots |
| p25 | Mean Intensity | BGC-Coloc | Red-Spots |
| p26 | Total Intensity | BGC-BFP | Coloc |
| p27 | Mean Intensity | BGC-BFP | Coloc |
| p28 | Total Intensity | BGC-TRITC | Coloc |
| p29 | Mean Intensity | BGC-TRITC | Coloc |
| p30 | Total Intensity | BGC-Coloc | Coloc |
| p31 | Mean Intensity | BGC-Coloc | Coloc |
| p32 | Area | | EGFP |
| p33 | Mean Intensity | Smoothing_EGFP | Main |

Measurement: Area

Color Channel: BFP

Object: Main

New | Remove

**k**

| |
|---|
| Sum Area Coloc Spots |
| Mean Intensity BFP Blue Spots |
| Mean Intensity TRITC Blue Spots |
| Mean Intensity "Coloc" Blue Spots |
| Mean Intensity BFP Red Spots |
| Mean Intensity TRITC Red Spots |
| Mean Intensity "Coloc" Red Spots |
| Mean Intensity BFP Coloc Spots |
| Mean Intensity TRITC Coloc Spots |
| Mean Intensity "Coloc" Coloc Spots |
| Calculated % Area Overlap Blue & Red Spots per MO |
| Calculated % Coloc-Area per Main Object Area |

Assay Settings

Main Object | Sub-objects | Parameters | Derived Parameters | Image Processing | Virtual Channels | Image Export

Derived Parameters

| ID | Name | Formula |
|---|---|---|
| D1 | Sum Area Blue Spots | SUM(p2) |
| D2 | Sum Area Red Spots | SUM(p3) |
| D3 | Sum Area Coloc Spots | SUM(p4) |
| D4 | Mean Intensity BFP Blue | SUM(p14)/SUM(p2)+1 |
| D5 | Mean Intensity TRITC B | SUM(p16)/SUM(p2)+1 |
| D6 | Mean Intensity "Coloc" | SUM(p18)/SUM(p2)+1 |
| D7 | Mean Intensity BFP Rec | SUM(p20)/SUM(p3)+1 |
| D8 | Mean Intensity TRITC R | SUM(p22)/SUM(p3)+1 |
| D9 | Mean Intensity "Coloc" | SUM(p24)/SUM(p3)+1 |
| D10 | Mean Intensity BFP Col | SUM(p26)/SUM(p4)+1 |
| D11 | Mean Intensity TRITC C | SUM(p28)/SUM(p4)+1 |
| D12 | Mean Intensity "Coloc" | SUM(p30)/SUM(p4)+1 |
| D13 | Calculated % Area Ove | SUM(p4)/(SUM(p2)+SUM(p3))*100 |
| D14 | Calculated % Coloc-An | SUM(p4)/(p1)*100 |

Name: Sum Area Blue Spots

Formula: SUM(), STDV(), MEAN()

SUM(p2)

Parameter Selector: No Selection

New | Remove

Image Selection for Module Adjustment | Wells | Positions | Timesteps

Reset | All | All | All

Compatibility Status

Cancel | OK



doi:10.6342/NTU201704022

## Figure 3. Detailed steps in ScanR Analysis

(a)The original images for the ScanR assay testing. Scale bars, 10μm.

(b)Magnified view of the EBFP2-Parkin and Anti-Ub regions (yellow rectangles in Fig. 2a). The co-localized area in Merge channel showed white signals. Scale bars, 10μm.

(c, d)The “Background correction” were applied to BFP and TRITC channels with the filter size=10.

(e) Signals of BGC-BFP, 10 folds of DEEPRED and BGC-TRITC channels were added, and applied to “Smoothing (median)” correction with Kernel Size=15 and Iteration=10. The output channel was for the cell area definition in Fig. 2h.

(f) The signals of BFP, DEEPRED and EGFP channels were added. The “Simple math” panel showed mathematical operators (＋, －, ×, ÷) and parameters (1~10) could be chosen.

(g) The BGC-BFP was multiplied by BGC-TRITC, and divided by white_1000 channel to obtain BGC-coloc channel, which was for co-localization analysis.

(h) The cell area was defined by setting the signal threshold in All_madian channel, and the output image showed the determined objects, which represented as single cell. (top). The intensity of Smoothing_EGFP channel was determined by setting low value of threshold to select large area of ROI (bottom).



doi:10.6342/NTU201704022

(i) The threshold of BGC-BFP, BGC-TRITC and BGC-coloc were set for characterizing the puncta. Images were the same region showed in Fig.2b.

(j) The parameter list in analyzing by ScanR.

(k) Derived parameters list in analyzing by ScanR, which “Names” (red rectangle) were listed in the table.



doi:10.6342/NTU201704022

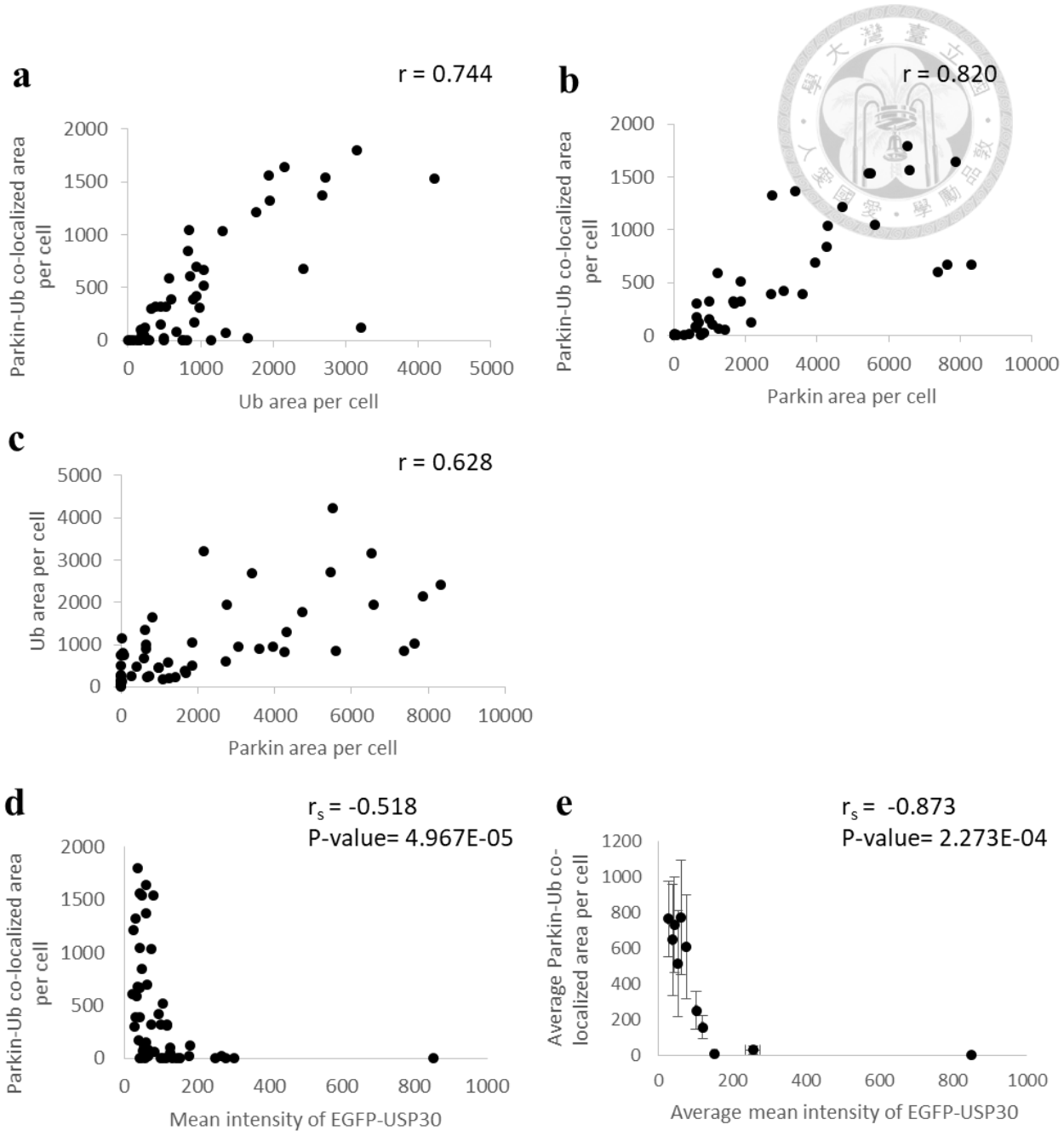


## Figure 4. The ScanR analysis assay is applicable on single cell measurement.

The scanR analysis results for Fig.2a. Cell number=51.

(a) Ub area per cell and Ub-Parkin co-localization area per cell have positive correlation with r = 0.744.



doi:10.6342/NTU201704022

(b) Parkin area per cell and Ub-Parkin co-localization area per cell have positive correlation with r = 0.820.

(c) Parkin area per cell and Ub area per cell have positive correlation with r = 0.628.

(d) Mean intensity of EGFP-USP30 and Ub-Parkin co-localization area per cell are negatively correlated with $r_s$= -0.518, P-value= 4.967E-05.

(e) The raw data in Fig. 3d were sorted. Each point represents a mean value from 5 cells measured. Error bars, SEM. The parameters showed negative correlation with $r_s$ = -0.873, P-value= 2.273E-04.



doi:10.6342/NTU201704022

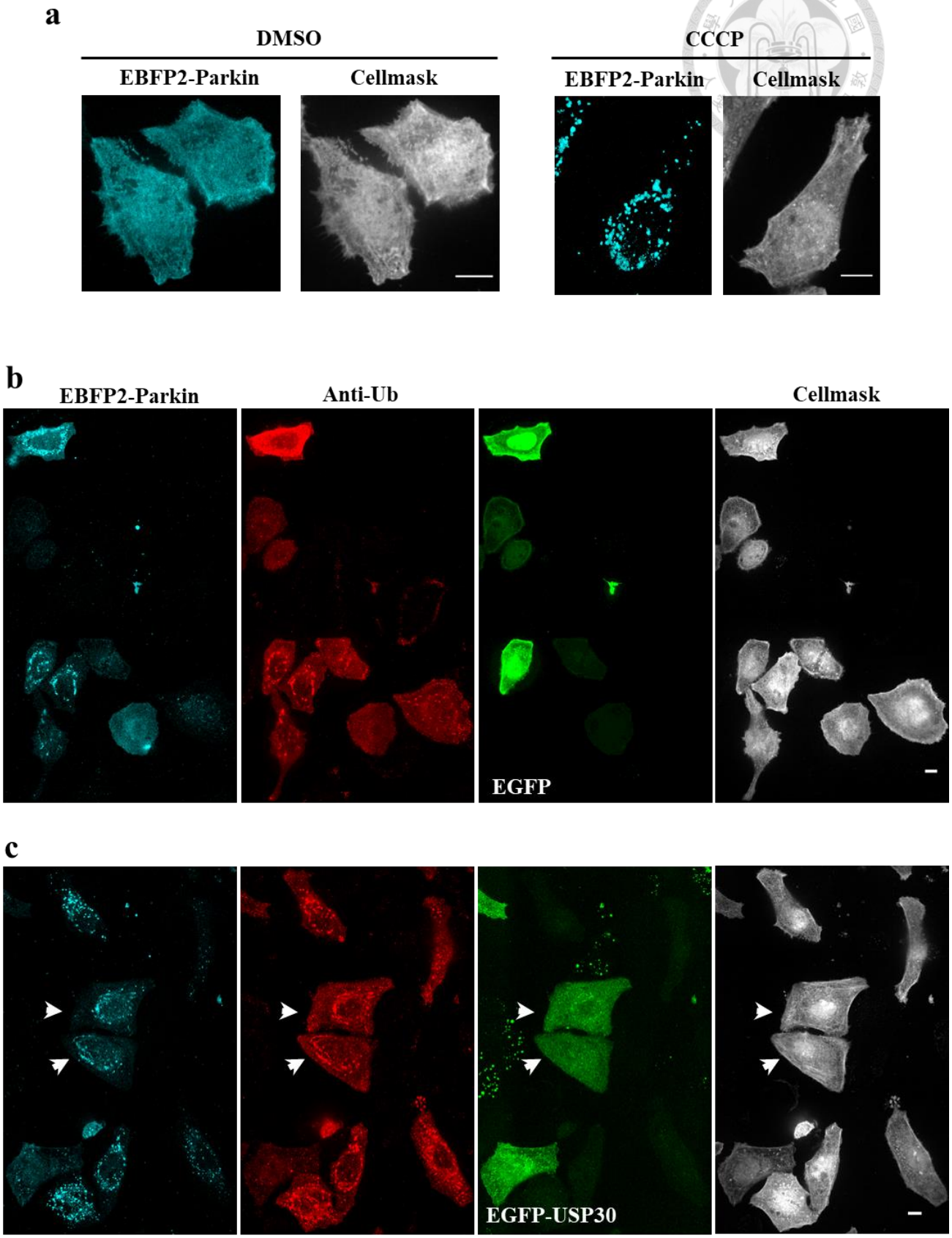




doi:10.6342/NTU201704022

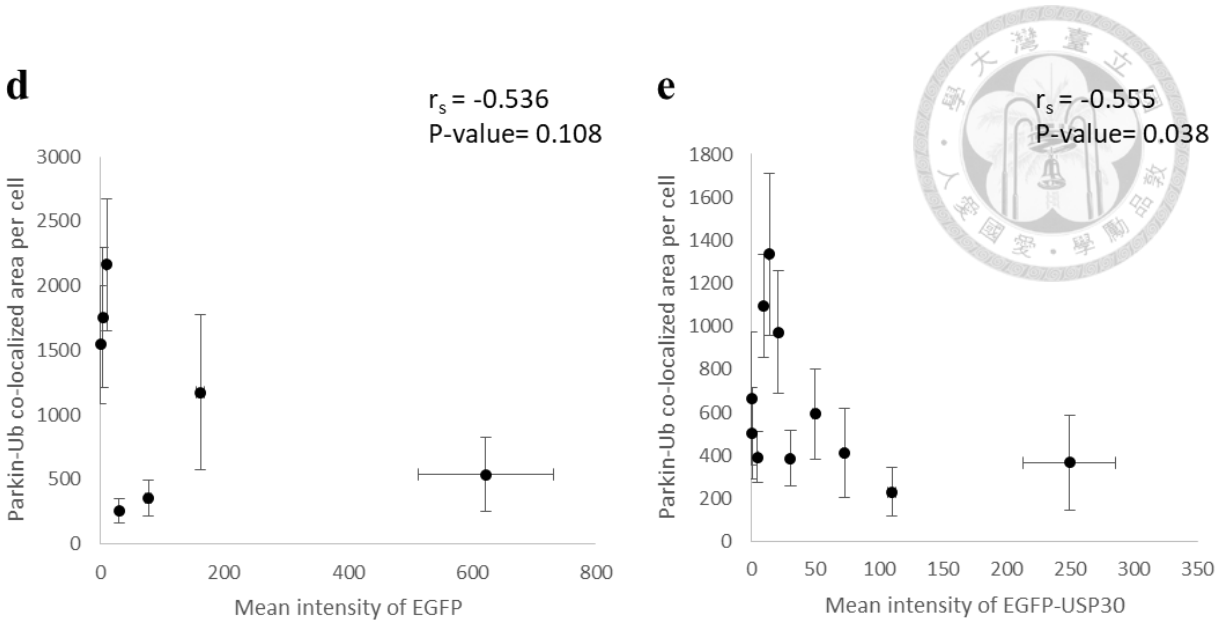


## Figure 5. The ScanR analysis assay test by larger amount of cells in mitophagy.

Assay testing with mitophagy induced by 10μM CCCP for 2 hr in HeLa cells. Scale bars, 10μm.

(a) Stable cells with EBFP2-Parkin were homogeneously distributed under normal condition, while EBFP2-Parkin was recruited under CCCP treatment.

(b) Cells were transfected with EGFP-C1 by lipofectamine as a control group (Cropped image section).

(c) Cells were transfected with EGFP-USP30 by lipofectamine (Cropped image section).

(d) Statistical analysis of experiment group from Fig.5a. The mean intensity of EGFP and Ub-Parkin co-localization area per cell were negatively correlated with $r_s$ = -0.536, P-value= 0.555. Total cell number = 171. Each point represents a mean value from 10~25



doi:10.6342/NTU201704022

cells measured. Error bars, SEM.

(e) Statistical analysis of experiment group from Fig.5b. The mean intensity of EGFP-USP30 and Ub-Parkin co-localization area per cell were negatively correlated with $r_s$ = -0.555, P-value= 0.038. Total cell number = 268. Each point represents a mean value from 10~25 cells measured. Error bars, SEM.



doi:10.6342/NTU201704022

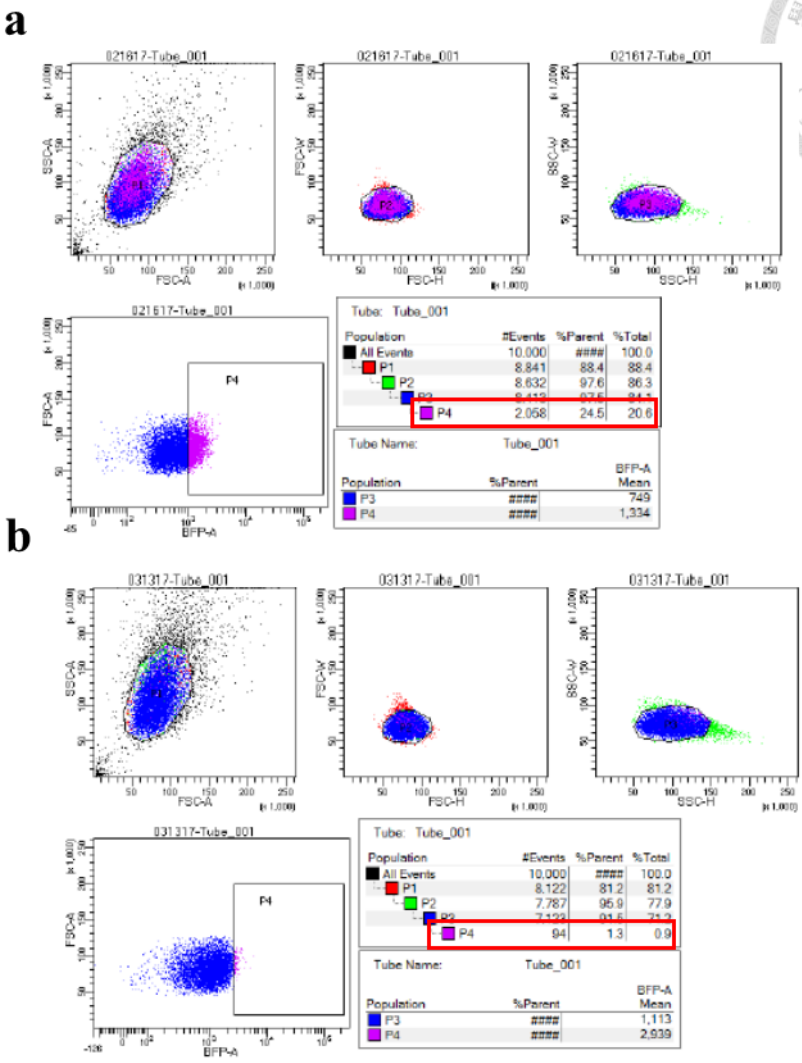


c

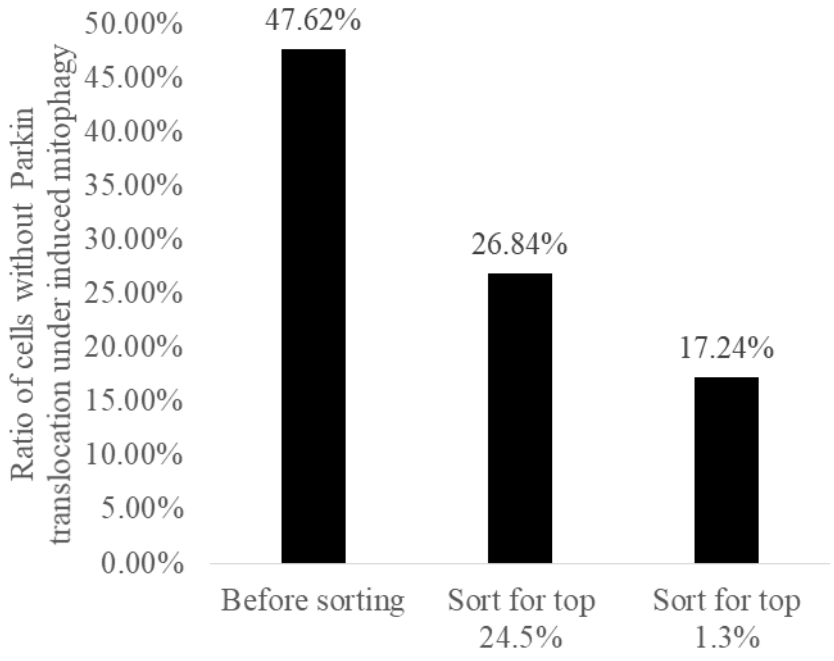




doi:10.6342/NTU201704022

## Figure 6. Sorting the HeLa EBFP2-Parkin stable cells.

(a) The cells were sorted by the EBFP2 intensity for top 24.5% cells by FACs.

(b) The cells were sorted by the EBFP2 intensity for top 1.3% cells by FACs.

(c) Three independent experiments with only induced mitophagy by CCCP or mitotracker along with illumination without transfecting any plasmids. The EBFP2-Parkin puncta area was calculated by ScanR assay, and defined that no Parkin translocation to damaged mitochondria when the area of EBFP2-Parkin <200 pixels. 47.62 % of cells showed no parkin translocation before sorting, and transferred to 26.84% and 17.64% after the first and second sorting, which respectively chose cells with the top 24.5% and top 1.3% EBFP2 intensity.



doi:10.6342/NTU201704022

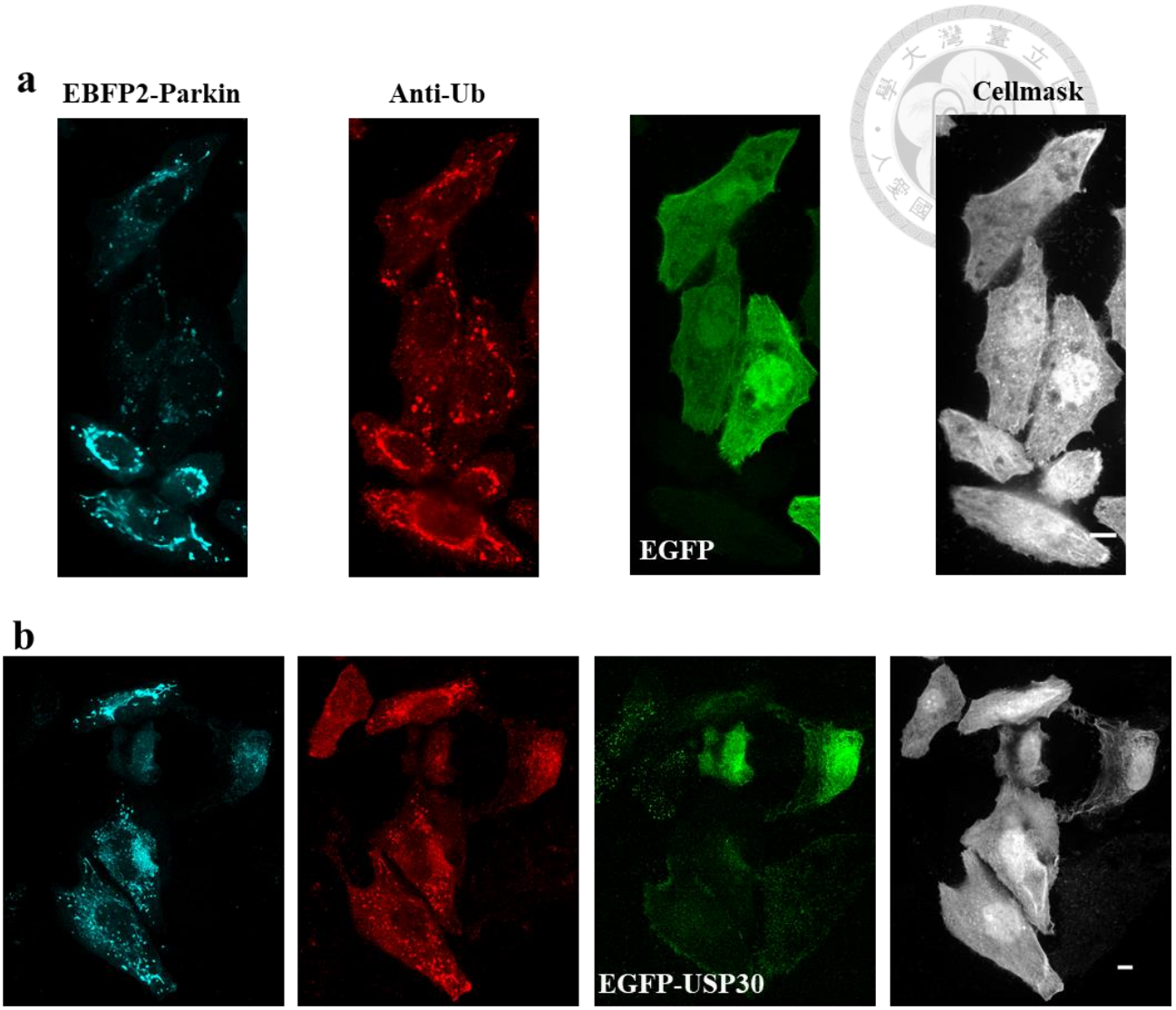




doi:10.6342/NTU201704022

## Figure 7. The ScanR analysis assay test by mitophagy from illuminated Mitotracker.

Assay testing with mitophagy induced by staining 200nM Mitotracker Deepred for 30 min along with illumination for 60 sec in HeLa cells. Scale bars, 10μm.

(a) Cells were transfected with EGFP-C1 by lipofectamine as a control group (Cropped image section).

(b) Cells were transfected with EGFP-USP30 by lipofectamine (Cropped image section).

(c) Statistical analysis of experiment group from Fig.7a. The mean intensity of EGFP and Ub-Parkin co-localization area per cell were negatively correlated with $r_s$ = -0.325, P-value= 0.119. Total cell number =356. Each point represents a mean value from 10~25 cells measured. Error bars represent SEM.

(d) Statistical analysis of experiment group from Fig.5b. The mean intensity of EGFP-USP30 and Ub-Parkin co-localization area per cell are negatively correlated with $r_s$= -0.412, P-value= 0.050. Total cell number = 427. Each point represents a mean value from 10~25 cells measured. Error bars, SEM.



doi:10.6342/NTU201704022

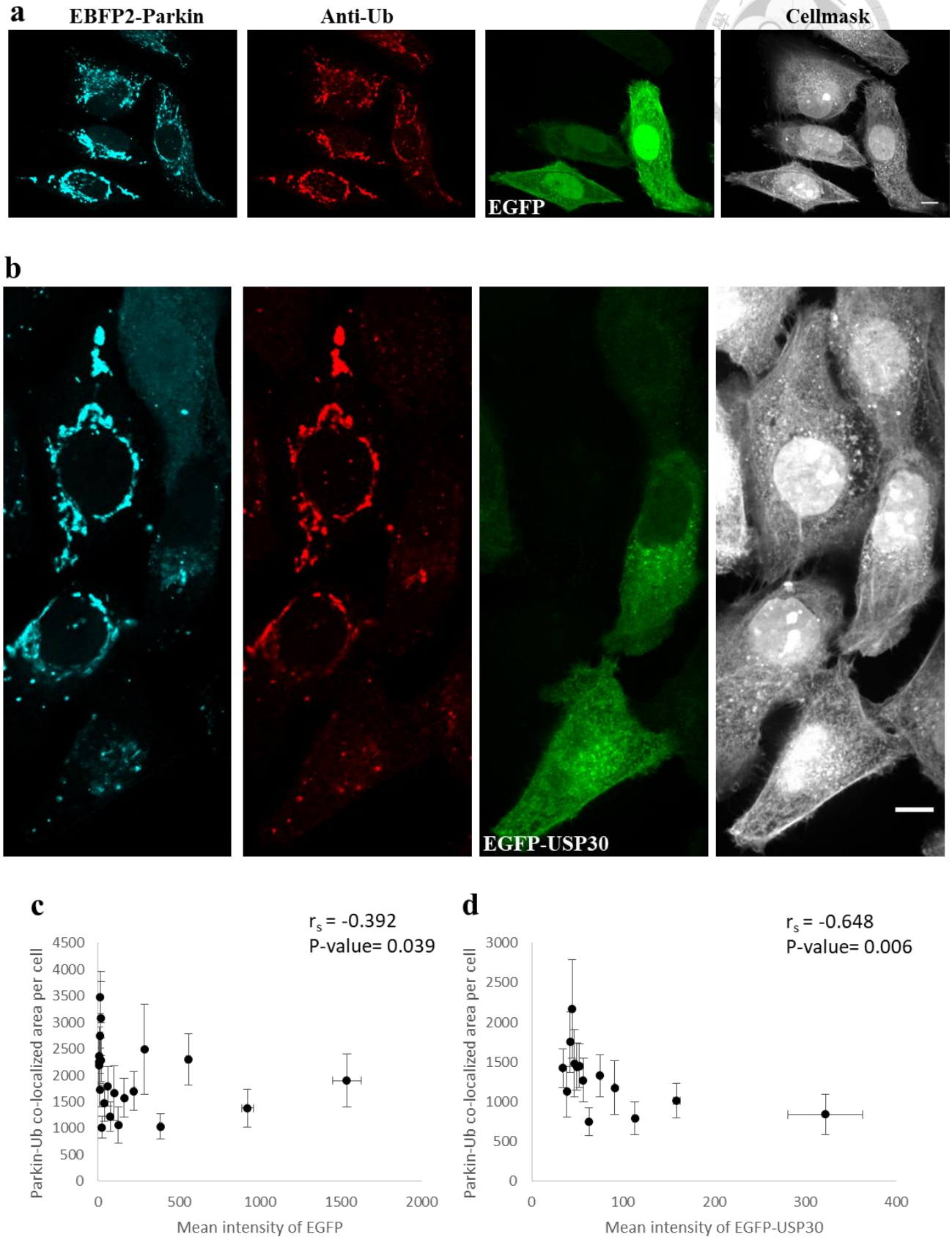




doi:10.6342/NTU201704022

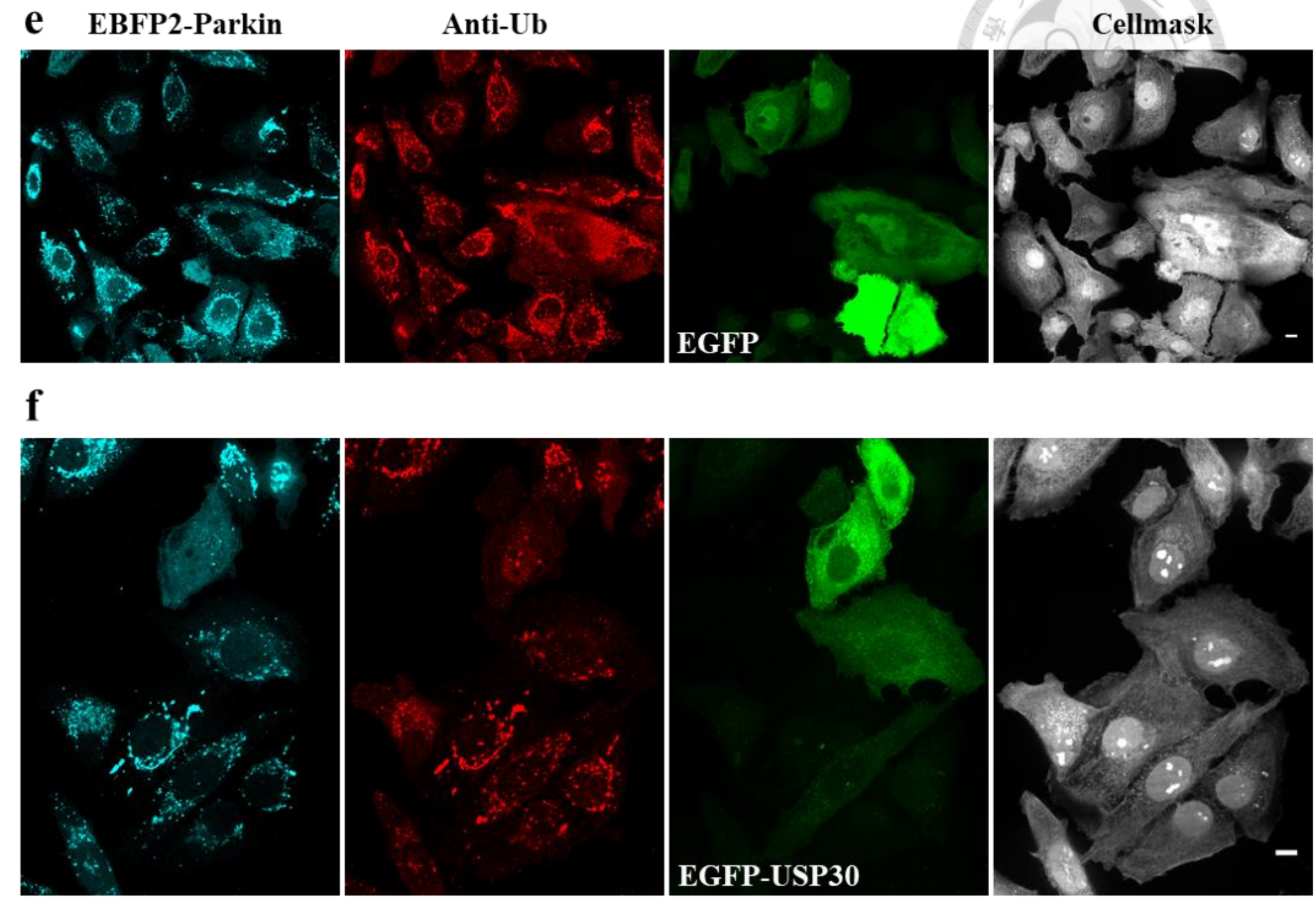


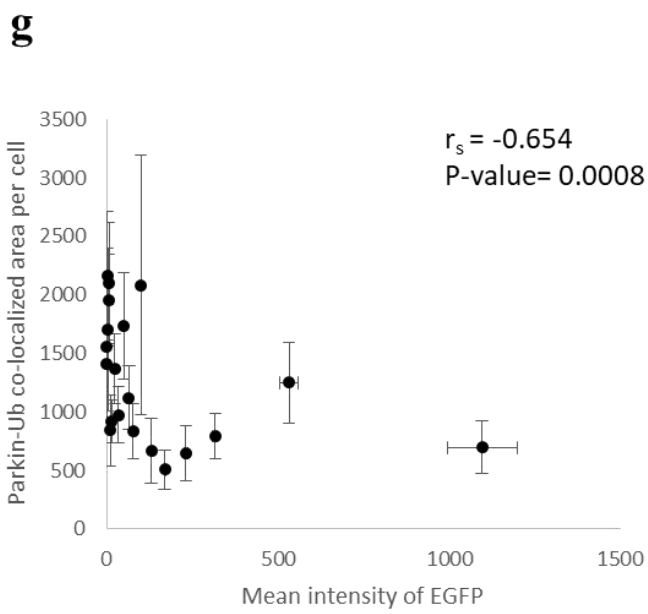


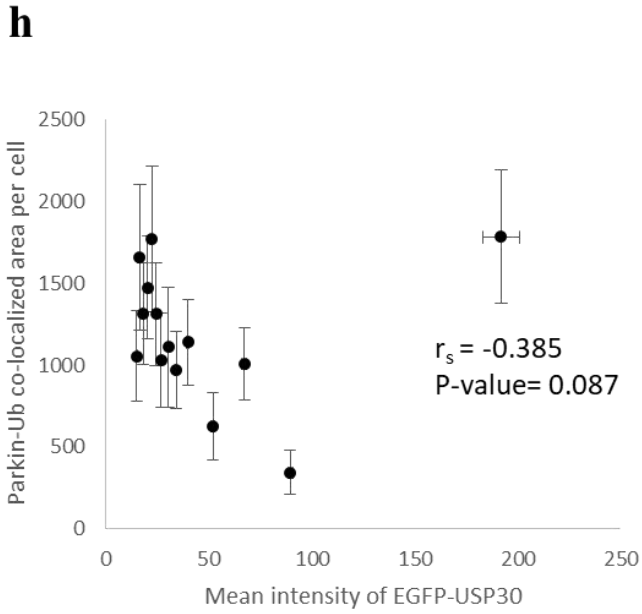




doi:10.6342/NTU201704022

## Figure 8. Change the transfection method to electroporation

Assay testing with mitophagy induced by treating 10μM CCCP for 2 hr or staining 200nM Mitotracker Deepred for 30 min along with illumination for 60 sec in HeLa cells. Scale bars, 10μm.

(a) Cells were transfected with EGFP-C1 as a control group by electroporation and induced mitophagy by illuminating Mitotracker (Cropped image section).

(b) Cells were transfected with EGFP-USP30 by electroporation and induced mitophagy by illuminating Mitotracker (Cropped image section).

(c) Statistical analysis of experiment group from Fig.8a. The mean intensity of EGFP and Ub-Parkin co-localization area per cell were negatively correlated with $r_s$ = -0.392, P-value= 0.039. Total cell number = 511. Each point represents a mean value from 10~25 cells measured. Error bars, SEM.

(d) Statistical analysis of experiment group from Fig.8b. The mean intensity of EGFP-USP30 and Ub-Parkin co-localization area per cell were negatively correlated with $r_s$ = -0.648, P-value= 0.006. Total cell number = 346. Each point represents a mean value from 10~25 cells measured. Error bars, SEM.

(e) Cells were transfected with EGFP-C1 as a control group by electroporation and induced mitophagy by CCCP (Cropped image section).



doi:10.6342/NTU201704022

(f) Cells were transfected with EGFP-USP30 by electroporation and induced mitophagy by CCCP (Cropped image section).

(g) Statistical analysis of experiment group from Fig.8f. The mean intensity of EGFP and Ub-Parkin co-localization area per cell were negatively correlated with $r_s$ = -0.654, P-value= 0.0008. Total cell number =468. Each point represents a mean value from 10~25 cells measured. Error bars, SEM.

(h) Statistical analysis of experiment group from Fig.8g. The mean intensity of EGFP-USP30 and Ub-Parkin co-localization area per cell were negatively correlated with $r_s$ = -0.385, P-value= 0.087. Total cell number = 354. Each point represents a mean value from 10~25 cells measured. Error bars, SEM.



doi:10.6342/NTU201704022

| PFA % | Fixation time | 4°C | RT | 37°C |
|---|---|---|---|---|
| 2% PFA | 10min | a 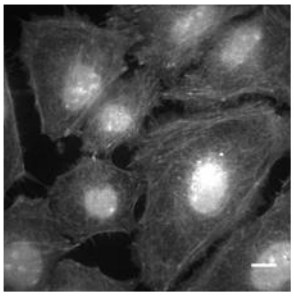 | b 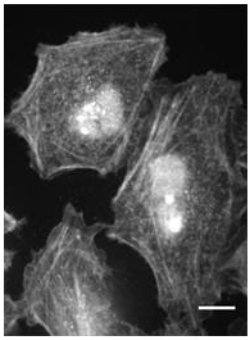 | |
| | 20min | c 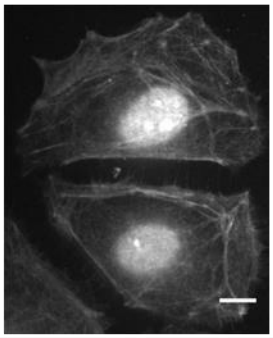 | d 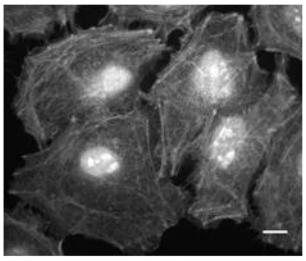 | e 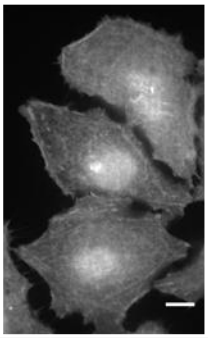 |
| 4% PFA | 5min | f 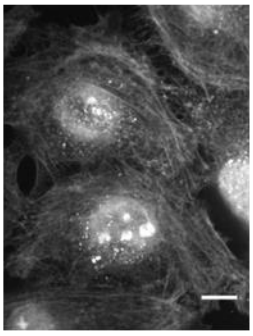 | g 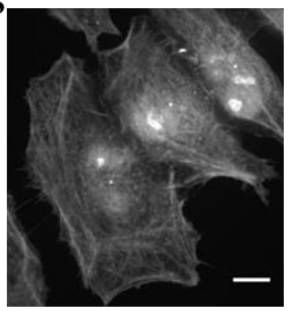 | h 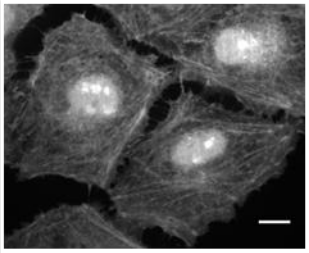 |
| | 10min | | i 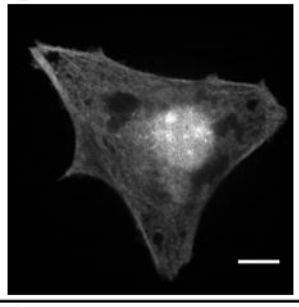 | |
| | 20min | | j 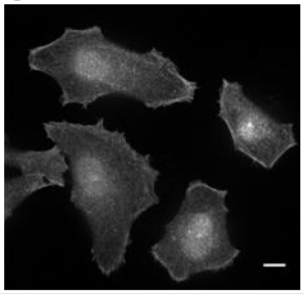 | k 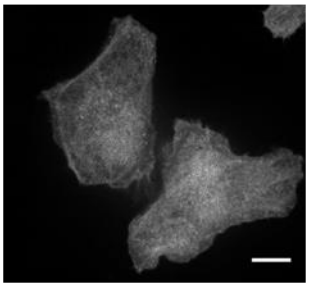 |



doi:10.6342/NTU201704022

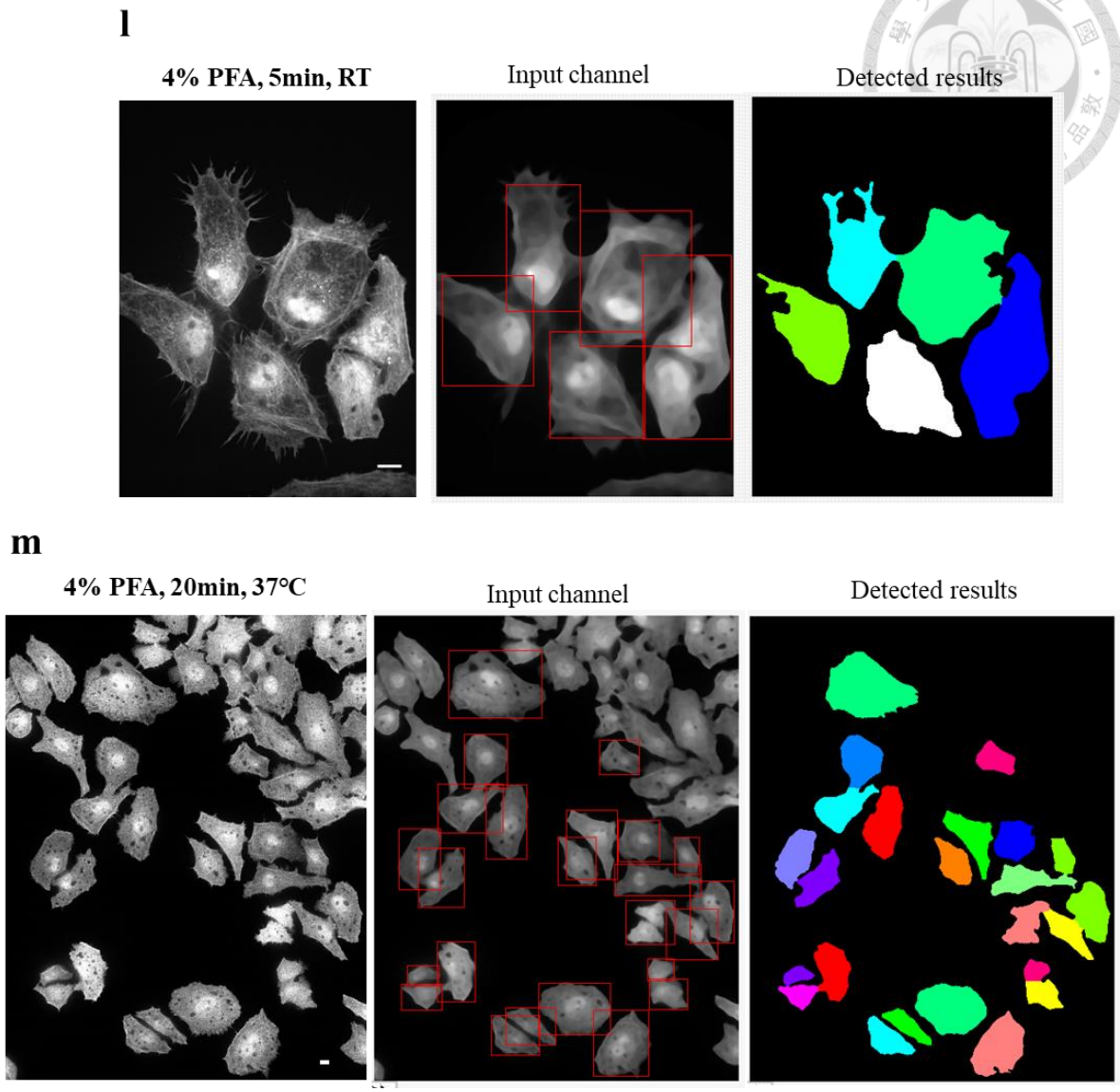


**Figure 9. Searching for the best conditions in fixation for ScanR analysis.**

(a~k) Different fixation condition with Cellmask stain for cells. 2% or 4% PFA were applied for various times (5, 10, 20 min) at three temperature settings (4℃, RT, 37℃). Scale bars, 10μm.



doi:10.6342/NTU201704022

(l) The cells from fixation of 4% PFA at RT for 5 min were segmented by scanR. Scale bars, 10μm.

(m) The cells from fixation of 4% PFA at 37℃ for 20 min were segmented by scanR. Scale bars, 10μm.



doi:10.6342/NTU201704022

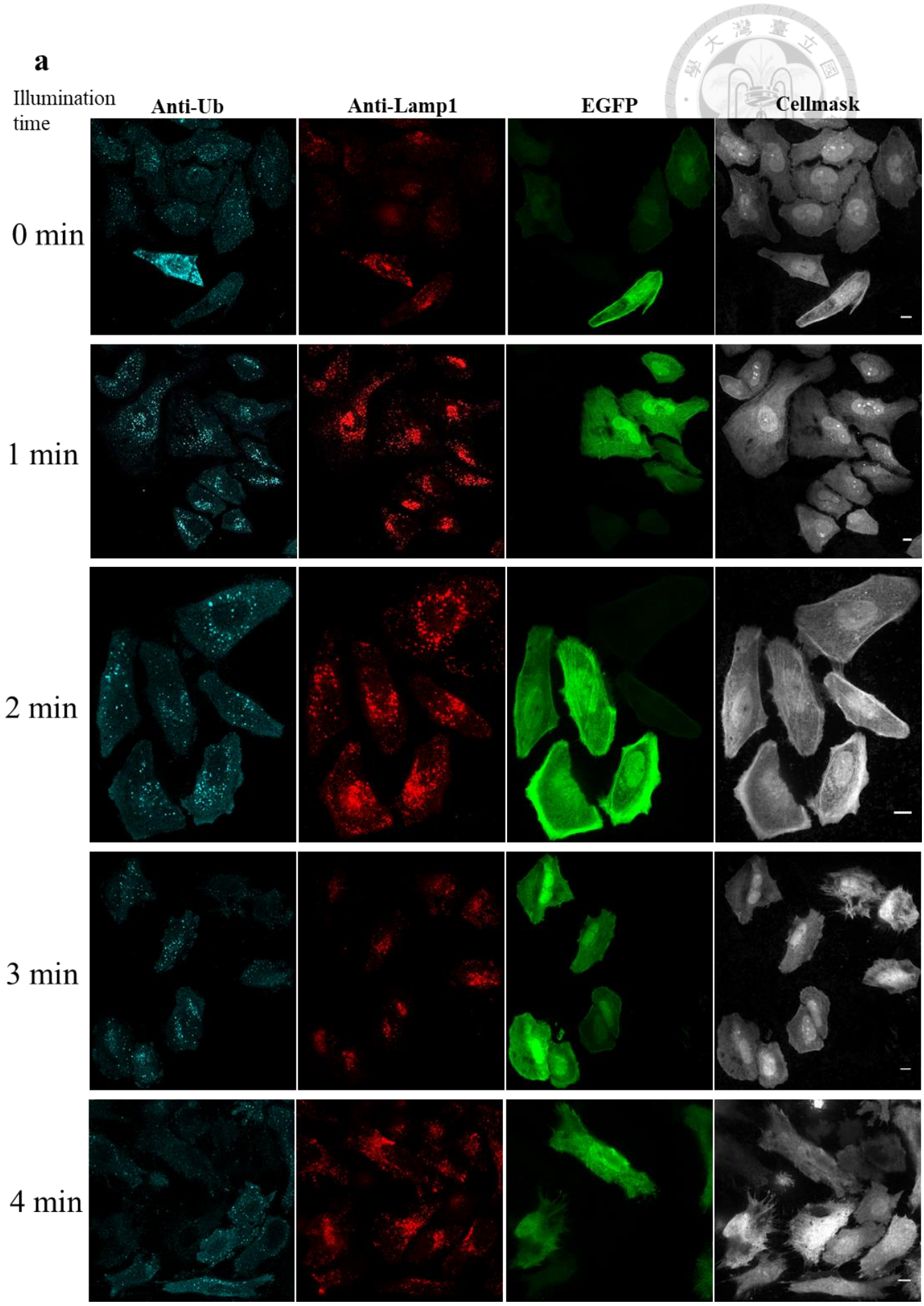




doi:10.6342/NTU201704022

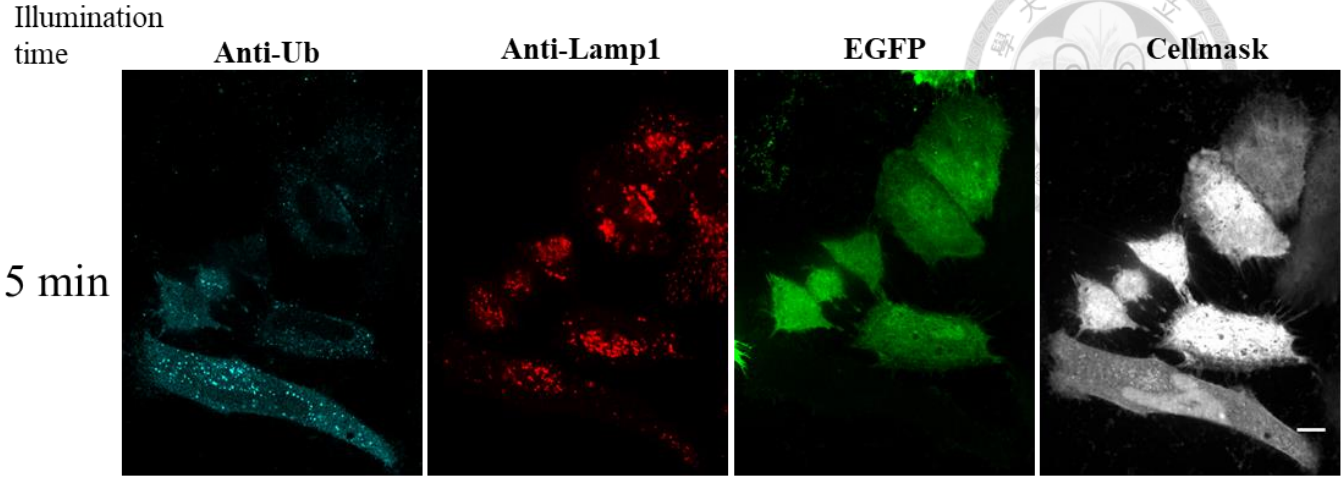


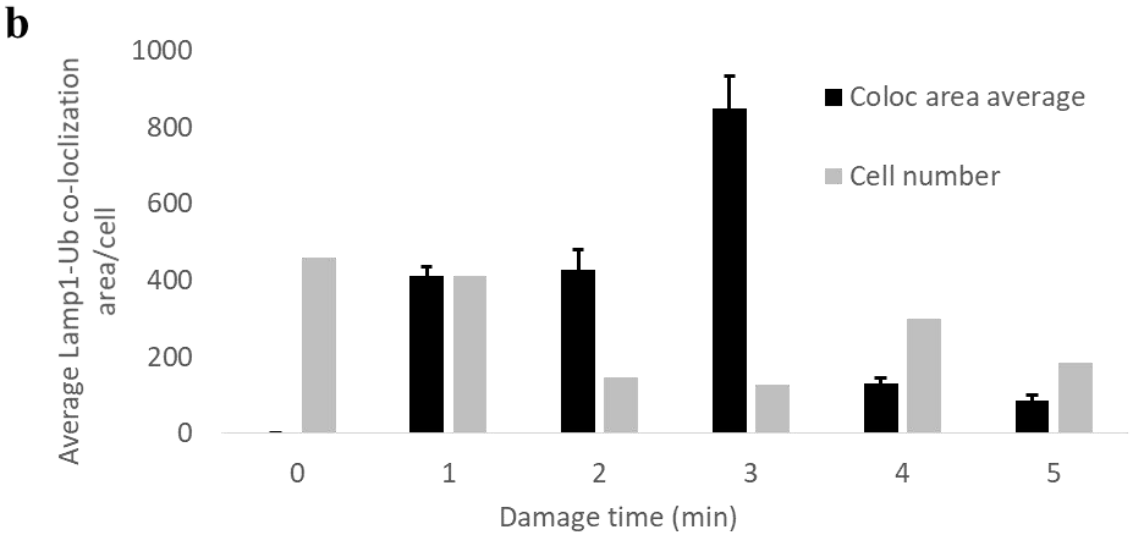


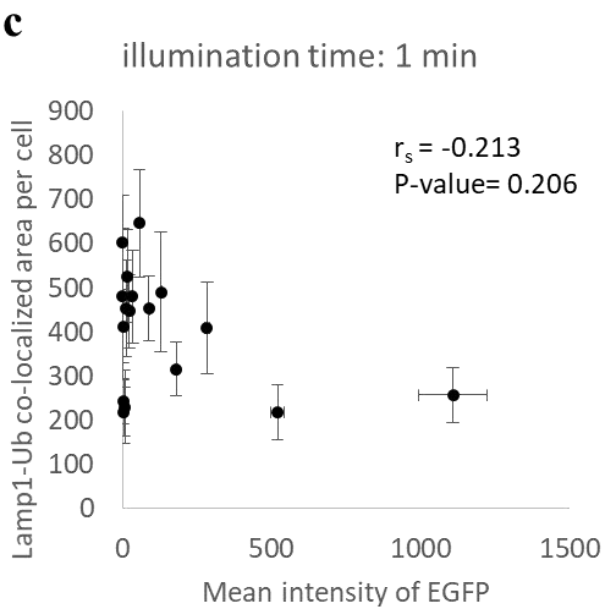


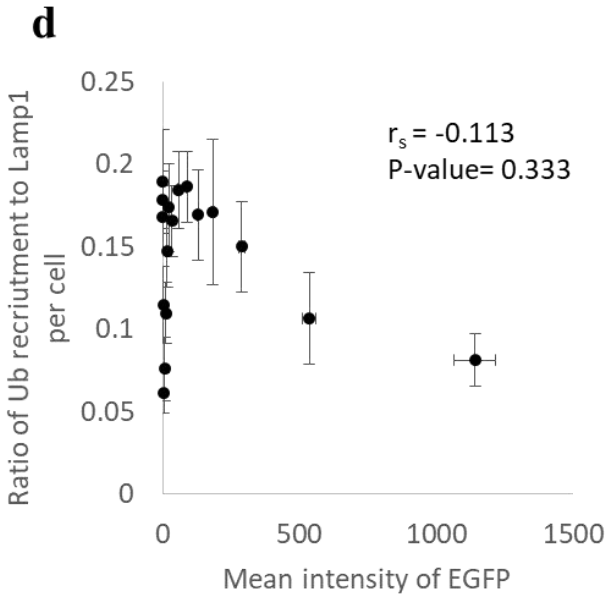




doi:10.6342/NTU201704022

## Figure 10. 1 min is the best illumination time for lysophagy

(a) HeLa cells were transfected EGFP by lipofectamine and induced lysophagy by illuminating AlPcS2a-stained cells with 650nm LED light. The images showed results from illuminating for 0, 1, 2, 3, 4, 5 min. Scale bars, 10μm.

(b) Average Ub-Lamp1 coloclization area/cell and cell number were listed in groups with each illumination time. Error bar, SEM.

(c) Statistical analysis of experiment group of 1-min illumination from Fig.10a. The mean intensity of EGFP and Ub-Parkin co-localization area per cell were negatively correlated with $r_s$ = -0.213, P-value= 0.206. Total cell number =410. Each point represents a mean value from 10~25 cells measured. Error bars, SEM.

(d) Statistical analysis of experiment group of 1-min illumination from from Fig.10a. The mean intensity of EGFP and ratio of Ub recruitment to Lamp1 per cell (Ub-Lamp1 co-localization area per cell/ Lamp1 area per cell) were negatively correlated with $r_s$ =-0.113, P-value=0.333. Total cell number = 410. Each point represents a mean value from 10~25 cells measured. Error bars, SEM.



doi:10.6342/NTU201704022

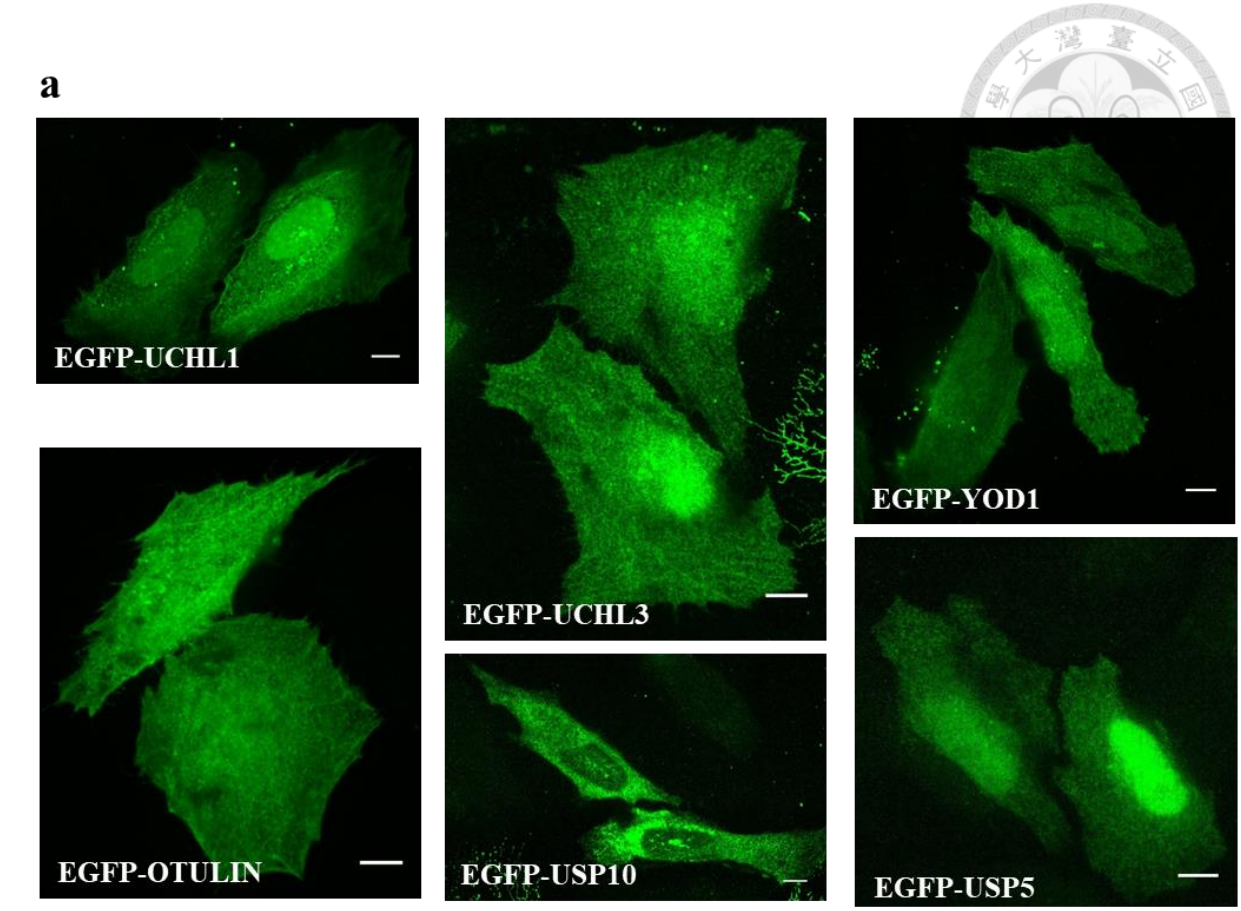


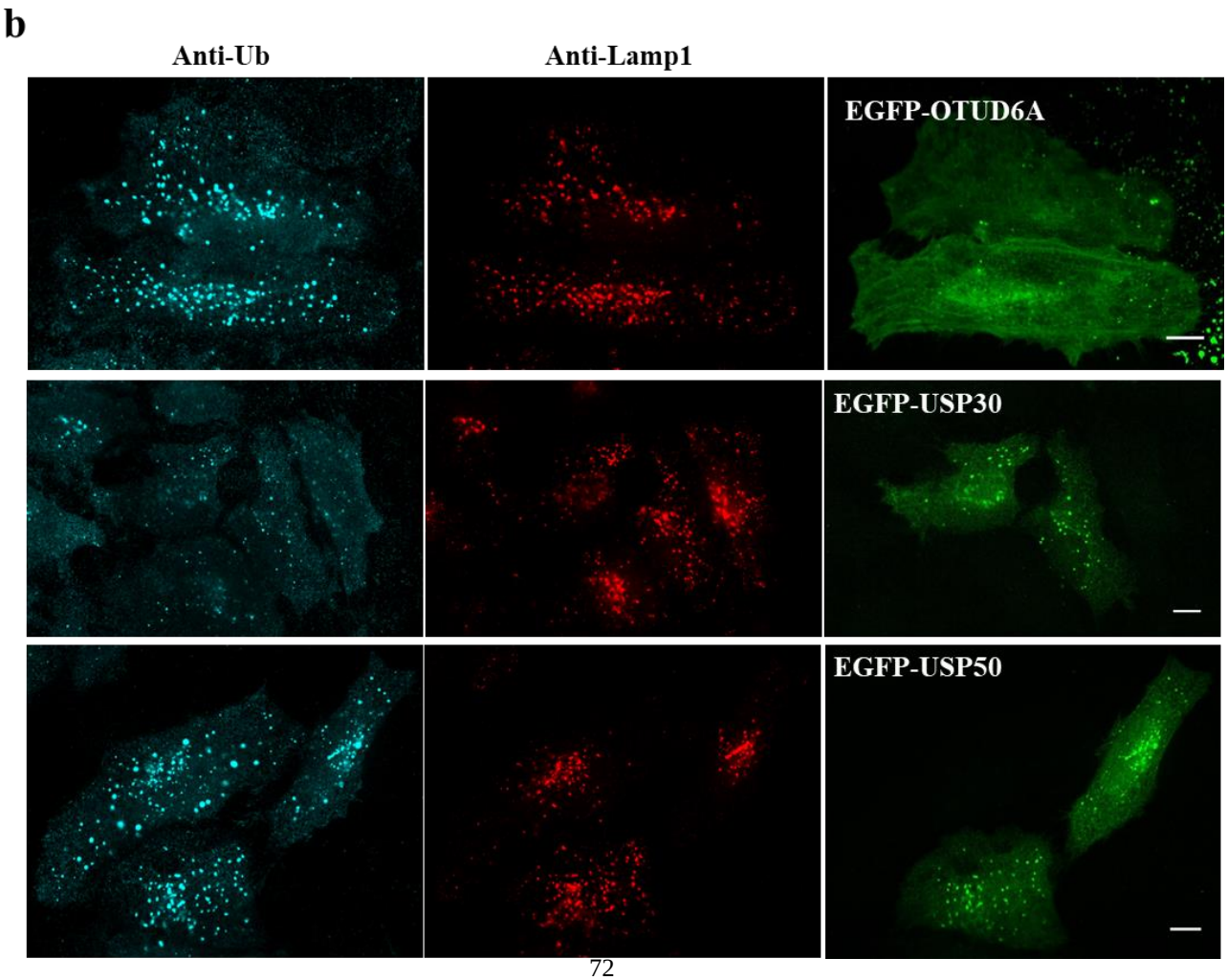




doi:10.6342/NTU201704022

**c**

| DUB | OTULIN | OTUD6A | UCHL1 | UCHL3 | USP5 | USP10 | USP30 | USP50 | YOD1 |
|---|---|---|---|---|---|---|---|---|---|
| N | 350 | 266 | 267 | 223 | 289 | 337 | 254 | 486 | 152 |
| $r_s$ | 0.187 | -0.718 | 0.136 | -0.117 | 0.455 | -0.705 | 0.127 | 0.534 | -0.086 |
| P-value | 0.739 | 0.006 | 0.655 | 0.383 | 0.931 | 0.002 | 0.645 | 0.992 | 0.436 |

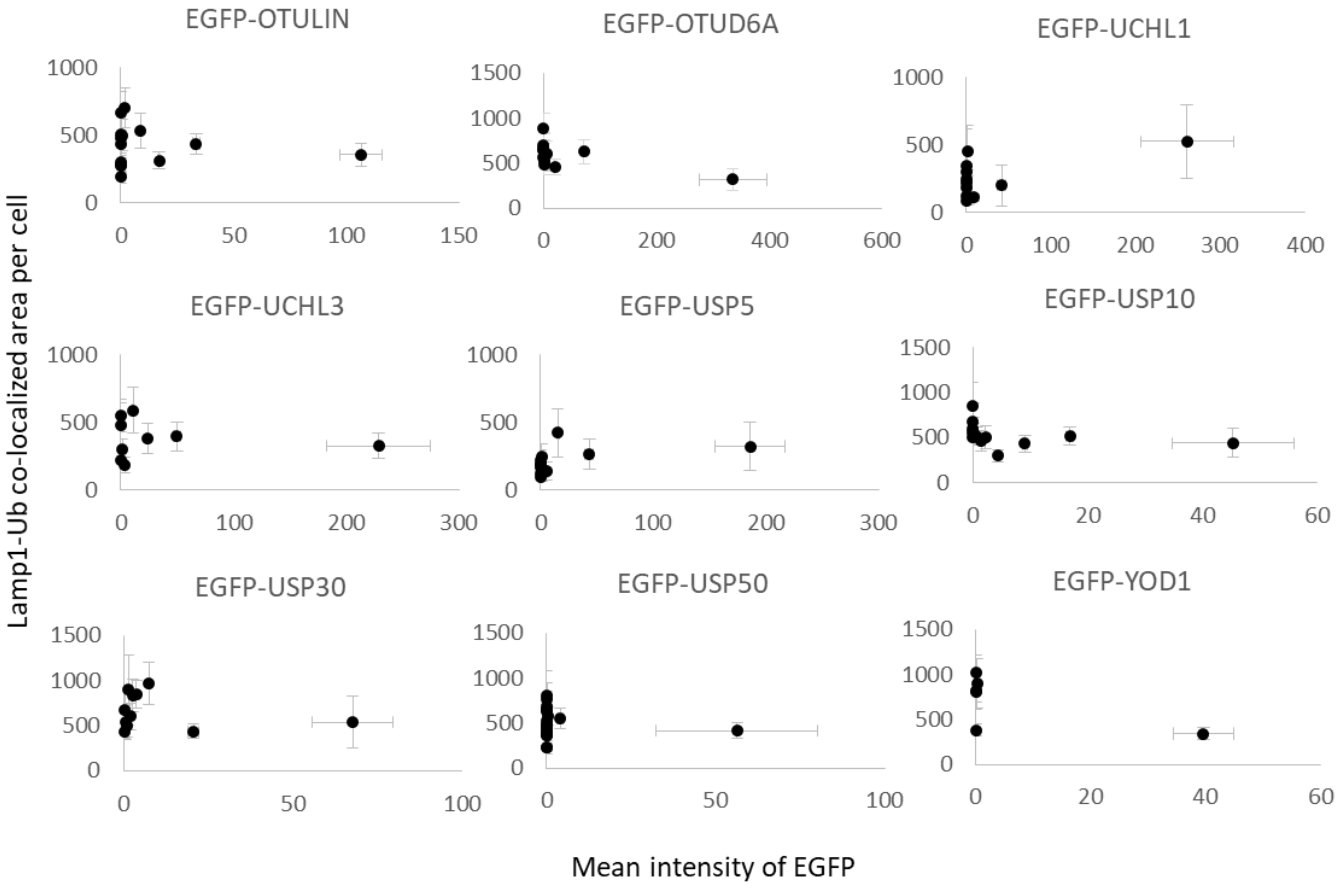


## Figure 11. OTUD6A and USP10 may be the candidates in reversing lysophagy.

(a) Cellular localization of the tested DUBs. Scale bar, 10μm.

(b) The DUBs showed co-localization with Ub or Lamp1 signals. Scale bar, 10μm.



doi:10.6342/NTU201704022

(c) Statistical analysis of the experiment group from Fig.11a, 11b. The correlation of mean intensity of EGFP and Ub/Lamp1 co-localization area per cell ($r_s$), P-value and total cell number (N) were listed in the table. Each point represents a mean value from 10~25 cells measured. Error bars, SEM.



doi:10.6342/NTU201704022

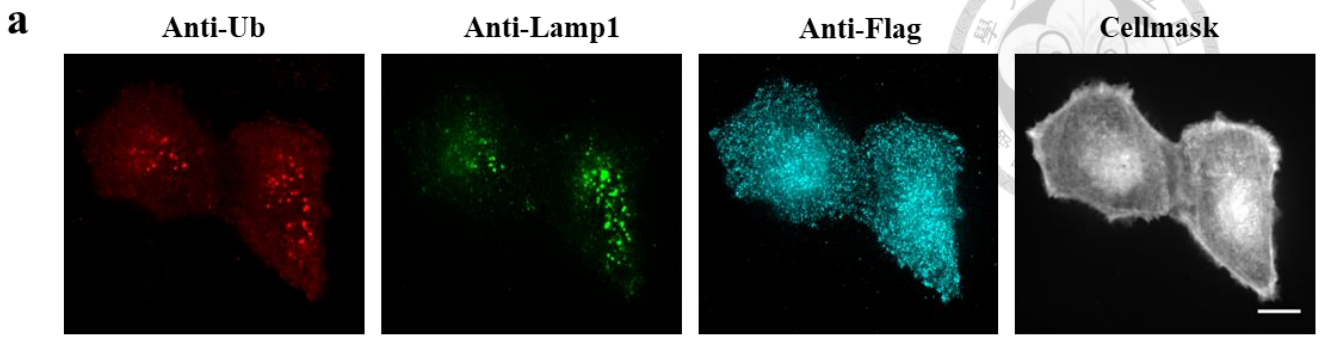


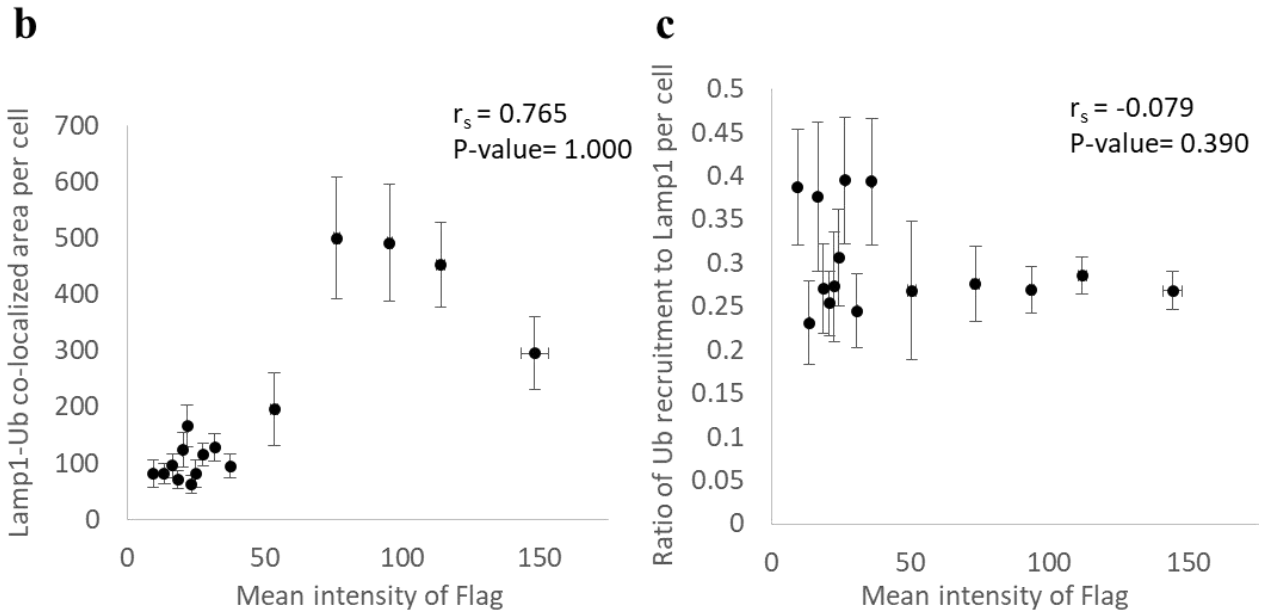


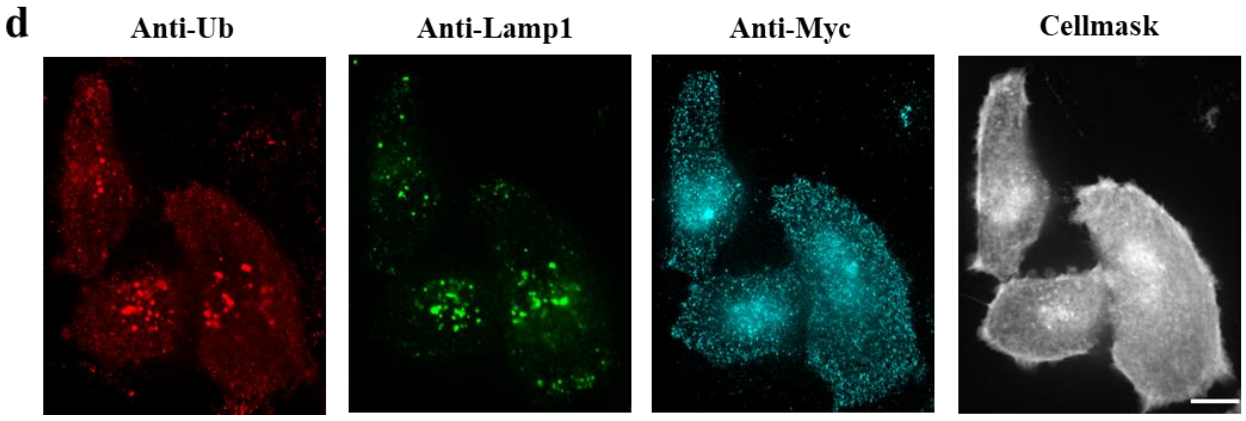




doi:10.6342/NTU201704022

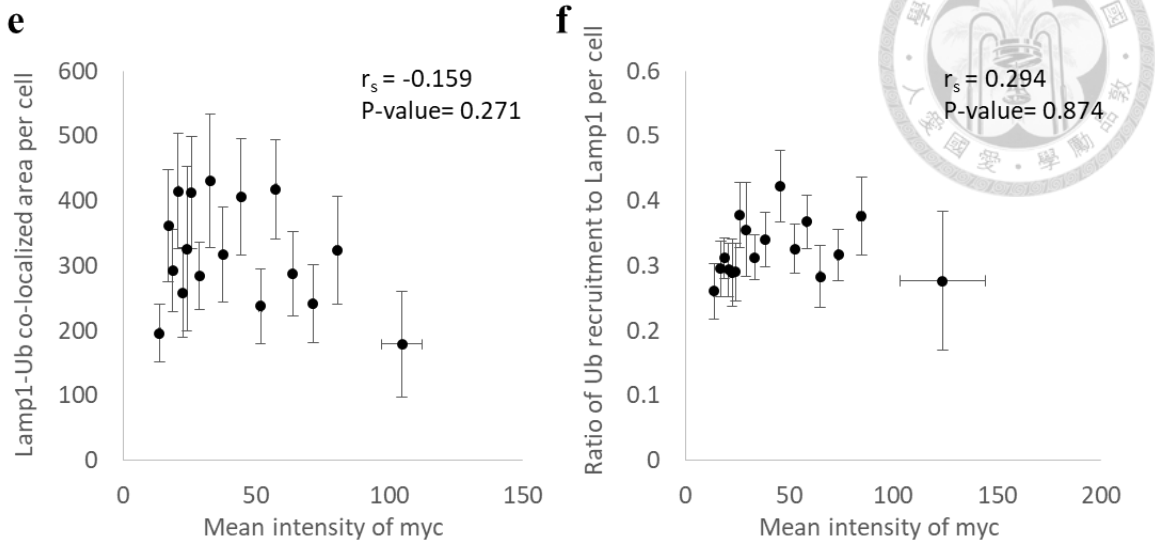


## Figure 12. Overexpression of tags in lysophagy.

(a) Cells were transfected with p3xFLAG-CMV™-7.1 by lipofectamine and induced lysophagy by illuminating AlPcS2a-stained cells with 650nm LED light for 1 min. (Cropped image section). Scale bars, 10μm.

(b) Statistical analysis of experiment group from Fig.13a. The mean intensity of Flag tags and Ub-Lamp1 co-localization area per cell were positively correlated with $r_s$ =0.765, P-value=1.000. Total cell number = 385. Each point represents a mean value from 15~25 cells measured. Error bars, SEM.

(c) Statistical analysis of experiment group from Fig.13a. The mean intensity of Flag tags and ratio of Ub recruitment to Lamp1 per cell (Ub-Lamp1 co-localization area per cell/ Lamp1 area per cell) were negatively correlated with $r_s$ =-0.079, P-value=0.390. Total cell number = 362 (some cells showed no lamp1 signals). Each point represents a mean value from 12~25 cells measured. Error bars, SEM.



doi:10.6342/NTU201704022

(d) Cells were transfected with pRK5-myc by lipofectamine and induced lysophagy by illuminating AlPcS2a-stained cells with 650nm LED light for 1 min. (Cropped image section). Scale bars, 10μm.

(e) Statistical analysis of experiment group from Fig.13d. The mean intensity of myc tags and Ub-Lamp1 co-localization area per cell were negatively correlated with $r_s$ =-0.159, P-value=0.271. Total cell number = 409. Each point represents a mean value from 9~25 cells measured. Error bars, SEM.

(f) Statistical analysis of experiment group from Fig.13d. The mean intensity of myc tags and ratio of Ub recruitment to Lamp1 per cell (Ub-Lamp1 co-localization area per cell/ Lamp1 area per cell) were positively correlated with $r_s$ =0.294, P-value=0.874. Total cell number = 403 (some cells showed no lamp1 signals). Each point represents a mean value from 10~25 cells measured. Error bars, SEM.



doi:10.6342/NTU201704022

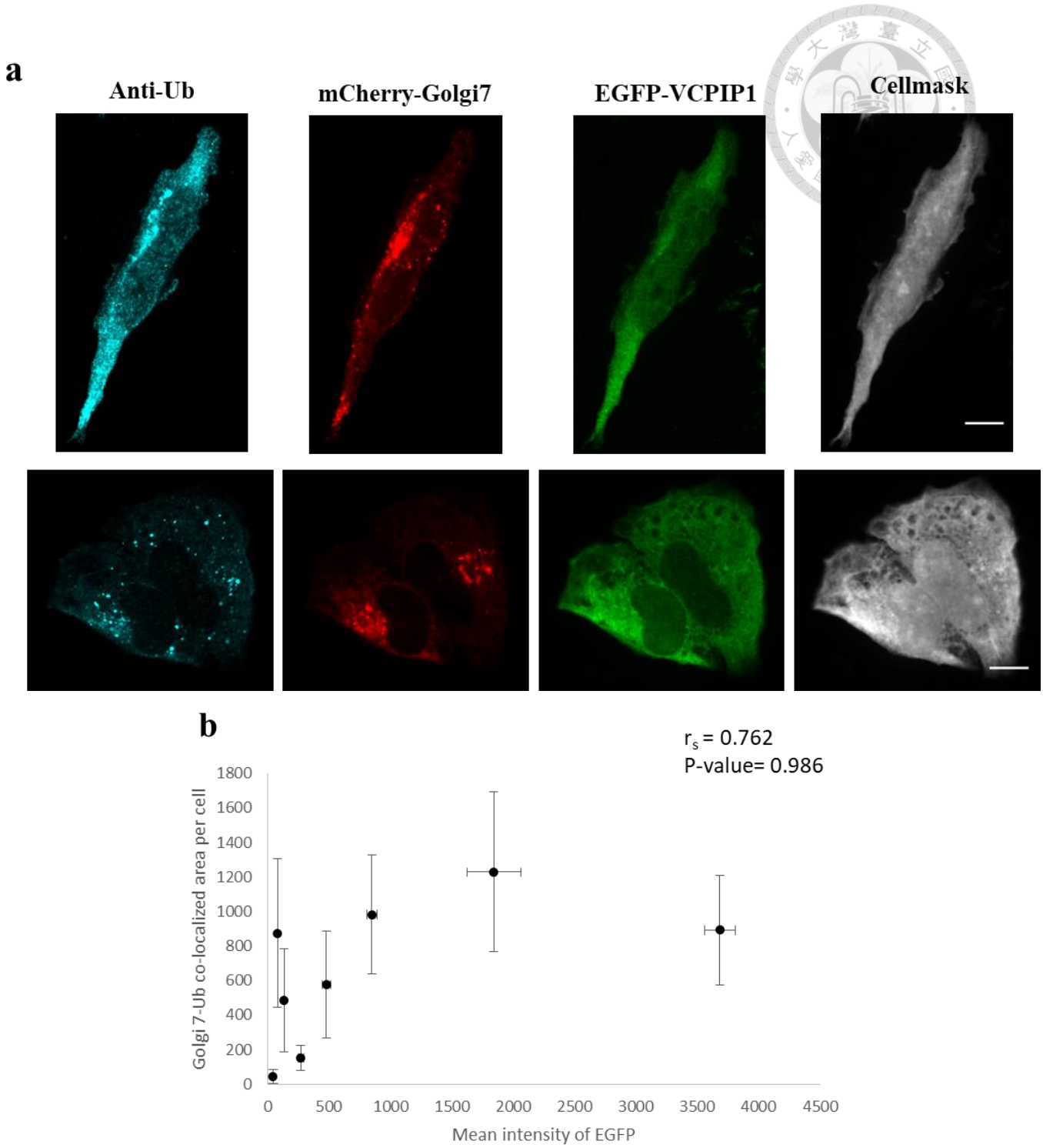


**Figure 13. VCPIP1 may not be the DUB for opposing Golgiphagy.**

(a) Cells were transfected with EGFP-VCPIP1 by lipofectamine and induced Golgiphagy by illuminating ZnPc (Cropped image section).



doi:10.6342/NTU201704022

(b) Statistical analysis of experiment group from Fig.11a. The mean intensity of EGFP-VCPIP1 and Ub-Golgi7 co-localization area per cell were positively correlated with $r_s$ =0.762, P-value=0.986. Total cell number = 78. Each point represents a mean value from 8~10 cells measured. Error bars, SEM.



doi:10.6342/NTU201704022

## Table 1. Information of plasmids

| Plasmids | Source | Catalog # | Restriction enzymes for EGFP-DUB cloning | References |
|---|---|---|---|---|
| Flag-HA-BRCC3 | Addgene | 22540 | HindIII / KpnI | (Sowa et al., 2009) |
| Flag-HA-JOSD3 | Addgene | 22549 | HindIII / SacII | (Sowa et al., 2009) |
| Flag-HA-OTUD5 | Addgene | 22610 | HindIII / KpnI | (Sowa et al., 2009) |
| Flag-HA-STAMBP | Addgene | 22560 | SacI / KpnI | (Sowa et al., 2009) |
| Flag-HA-UCHL1 | Addgene | 22563 | SacI / HindIII | (Sowa et al., 2009) |
| Flag-HA-UCHL3 | Addgene | 22564 | SacI / HindIII | (Sowa et al., 2009) |
| Flag-HA-USP5 | Addgene | 22590 | HindIII / KpnI | (Sowa et al., 2009) |
| Flag-HA-USP10 | Addgene | 22543 | SacI / SacII | (Sowa et al., 2009) |
| Flag-HA-USP15 | Addgene | 22570 | SacI / SacII | (Sowa et al., 2009) |
| Flag-HA-USP18 | Addgene | 22572 | SacI / KpnI | (Sowa et al., 2009) |
| Flag-HA-USP30 | Addgene | 22578 | KpnI / BamHI | (Sowa et al., 2009) |
| Flag-HA-USP50 | Addgene | 22588 | SacI / KpnI | (Sowa et al., 2009) |
| Flag-HA-VCPIP1 | Addgene | 22592 | BglII / SacII | (Sowa et al., 2009) |
| Flag-HA-YOD1 | Addgene | 22554 | HindIII / | (Sowa et al., 2009) |



doi:10.6342/NTU201704022

| | | | | |
|---|---|---|---|---|
| | | | BamHI | |
| p3xFLAG-CMV™-7.1 | Sigma | E4026 | - | A gift from Dr. Ruey-Hwa Chen's lab |
| pEGFP-C1 | Clontech | - | - | - |
| pEGFP-C1-A20 | Addgene | 22141 | - | (Li et al., 2008) |
| pOPINB-OTULIN | Addgene | 61464 | HindIII / KpnI | (Keusekotten et al., 2013) |
| pOPINK-OTUD6A | Addgene | 61416 | SacI / KpnI | (Mevissen et al., 2013) |
| pRK5-myc | Clontech | - | - | A gift from Dr. Ruey-Hwa Chen's lab |
| USP12 | Origene | SC127906 | HindIII / SacII | - |
| USP19-Flag/pRK5 | Addgene | 36306 | - | (Mei et al., 2011) |
| USP25 | Origene | SC115248 | SacI / SacII | - |
| mCherry-Golgi7 | - | - | - | - |



doi:10.6342/NTU201704022

## Table 2. PCR reaction conditions.

- **For DUB plasmids (insert fragments)**

| *Components* | *Volume (μl)* |
|---|---|
| Phusion Flash High-Fidelity PCR Master Mix (F548L) | 25 |
| Forward primer (25 μM) | 1 |
| Reverse primer (25 μM) | 1 |
| Templates (10ng/μl) | 1 |
| Sterilized dd$H_2O$ | 19.5 |
| DMSO | 2.5 |
| *Total volume* | *50* |

| Cycle steps | Temperature (℃) | Time | cycles |
|---|---|---|---|
| Initiation | 98 | 2 min. | 1 |
| Denaturation | 98 | 20 sec. | 30 |
| Annealing | By Tm calculator*<br>-0.1℃/cycle | 1 min. | |
| Extension | 72 | 1Kb/30 sec. | |
| Final elongation | 72 | 5 min. | 1 |
| Final hold | 4 | Until the machine was off manually | 1 |



doi:10.6342/NTU201704022

- **For cloning colony size check**

| *Components* | *Volume (μl)* |
|---|---|
| Ultra-Pure Taq PCR Master Mix | 5 |
| Forward primer (EGFP-C1-CMV, 25 μM) | 1 |
| Reverse primer (EGFP-C1-MCS, 25 μM) | 1 |
| Templates | A dip of E.coli colony |
| Sterilized dd$H_2O$ | 17 |
| DMSO | 1 |
| *Total volume* | *25* |

| Cycle steps | Temperature (℃) | Time | cycles |
|---|---|---|---|
| Initiation | 94 | 5 min | 1 |
| Denaturation | 94 | 1 min. | 25 |
| Annealing | By Tm calculator*<br>-0.1℃/cycle | 1 min. | |
| Extension | 72 | 1Kb/1 min. | |
| Final elongation | 72 | 10 min. | 1 |
| Final hold | 4 | Until the machine was off manually | 1 |



doi:10.6342/NTU201704022

- **For site directed mutagenesis (nucleotides insertion, deletion or point mutation)**

| *Components* | *Volume (μl)* |
|---|---|
| Phusion Flash High-Fidelity PCR Master Mix (F531L) | 25 |
| Phosphate forward primer (25 μM) | 4.5 |
| Phosphate reverse primer (25 μM) | 4.5 |
| Templates (10ng/μl) | 1 |
| Sterilized dd$H_2O$ | 14 |
| DMSO | 1 |
| *Total volume* | *50* |

| Cycle steps | Temperature (℃) | Time | cycles |
|---|---|---|---|
| Initiation | 98 | 30 sec.. | 1 |
| Denaturation | 98 | 10 sec. | 30 |
| Annealing | By Tm calculator* -0.1℃/cycle | 1 min. | |
| Extension | 72 | 1Kb/30 sec. | |
| Final elongation | 72 | 5 min. | 1 |
| Final hold | 4 | Until the machine was off manually | 1 |

***Tm calculator from ThermoFisher:**

(https://www.thermofisher.com/tw/zt/home/brands/thermo-scientific/molecular-biology/molecular-biology-learning-center/molecular-biology-resource-library/thermo-scientific-web-tools/tm-calculator.html)



doi:10.6342/NTU201704022

**Table 3. The conditions of enzyme digestion, restriction fragments ligation and primers phosphorylation reaction.**

- **Enzyme digestion**

| *Components* | *Volume (μl)* |
|---|---|
| DNA fragments from PCR (eluted by gel extraction kit) | 34 |
| Enzyme I | 1 |
| Enzyme II | 1 |
| Buffer for enzyme I & II (CutSmart were often used) | 4 |
| *Total volume* | *40* |

| *Components* | *Volume (μl)* |
|---|---|
| EGFP-C1 (total 1μg) + Sterilized dd$H_2O$ | 34 |
| Enzyme I | 1 |
| Enzyme II | 1 |
| Buffer for enzyme I & II (CutSmart were often used) | 4 |
| *Total volume* | *40* |



doi:10.6342/NTU201704022

- **Rrestriction fragments ligation**

| *Components* | *Volume (μl)* |
|---|---|
| Insert fragments + Vector fragments | 4 |
| 10X T4 ligase buffer | 0.5 |
| T4 ligase | 0.5 |
| *Total volume* | *5* |

- **primers phosphorylation reaction**

| *Components* | *Volume (μl)* |
|---|---|
| Primers (25 μM) | 12 |
| 10X T4 ligase buffer | 5 |
| Sterilized dd$H_2O$ | 32 |
| T4 PNK | 1 |
| *Total volume* | *50* |



doi:10.6342/NTU201704022

## Table 4. The laser conditions for imaging

| Excitation wavelength (nm) | Collecting emission wavelengths (nm) | Laser intensity (mW) (100%) | Laser intensity when imaging (mW) | Fluorescence emission in the study |
|---|---|---|---|---|
| 405 | 420~460 | 0.49 | 0.392 (80%) | EBFP2, Alexa 405 |
| 488 | 500~550 | 1.66 | 1.162 (70%) | EGFP , Alexa 488 |
| 561 | 580~620 | 2.07 | 0.621 (30%) | mCherry, Alexa 546 |
| 640 | 665~735 | 4.20 | 0.420 (1%) | Cellmask stain |



doi:10.6342/NTU201704022

## Table 5. Detailed steps in ScanR Analysis

### 1. For converting the files into “experiment_descriptor .XML”

| WINDOW SECTION | COMMENTS | SOFTWARE PANEL |
|---|---|---|
| Main window | *Scan→Custom conversion* | - |
| Image list | Select files from directory<br>“Retrive image list” button | 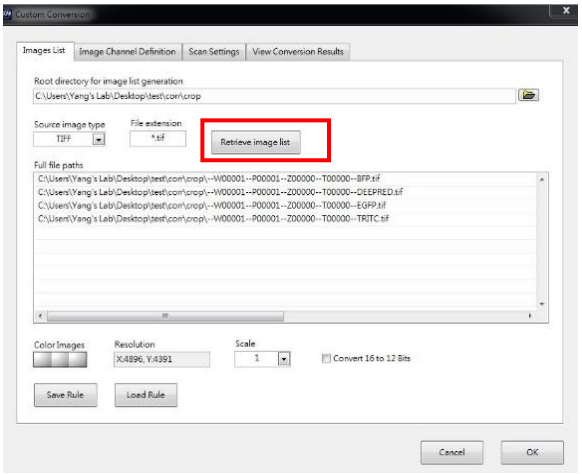 |
| Image channel definition | ● Define the channel names<br>● Files names only increase P number (position) between batches | 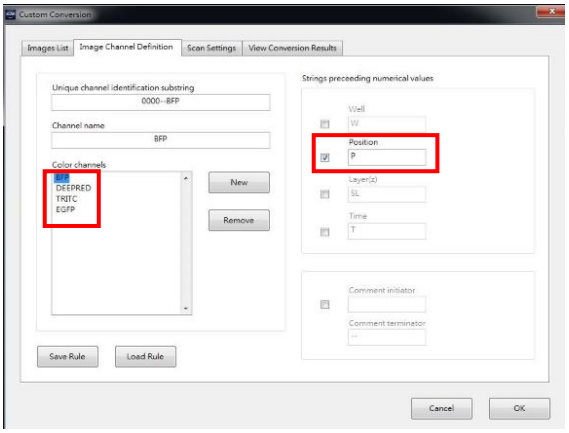 |
| Scan settings | Select result directory (The directory must be empty) | - |
| View conversion result | “Test”button →”start” button →”OK”button | - |



doi:10.6342/NTU201704022

## 2. For virtual channel settings explanation

| WINDOW SECTION | COMMENTS | INPUT CHANNEL | FACTOR | OUTPUT CHANNEL | SOFT-WARE PANEL |
|---|---|---|---|---|---|
| Main window | *Analysis→ Assay Settings* | - | | | |
| Virtual channel | Background correction | BFP | ▪Filter size=10<br>▪Dark background | BGC-BFP | Fig.3c |
| | | TRITC | | BGC-TRITC | Fig.3d |
| | Smoothing | EGFP | sigma=0.5 | Smoothing_EGFP | - |
| | Simple math | (BGC-BFP) + (10xDEEPRED) + (BGC-TRITC) | | All | |
| | Smoothing (Median) | All | ▪Kernel size=15<br>▪Iteration=10 | All-Median | Fig.3e |
| | Simple math | ❶❷BFP + DEEPRED + EGFP | | Forget-this-one & Forget-this-too | Fig.3f |
| | (only 3 channels can be calculated at a time) | ❸(Forget-this-one ) + TRITC | | SUNAllChannels_1 | - |
| | | ❹(Forget-this-too ) + TRITC | | SUNAllChannels_2 | |
| | | ❺(SUNAllChannels_1) ÷ (SUNAllChannels_2) | | White_01 | |
| | | ❻White_01 × (10xWhite_01) | | White_10 | |
| | | ❼White_10 × (10xWhite_10) | | White_1000 | |
| | | ❽(BGC-BFP) × (BCG-TRITC) ÷ (white_1000) | | BGC-coloc | Fig.3g |



doi:10.6342/NTU201704022

# References

Adler, J., and Parmryd, I. (2010). Quantifying Colocalization by Correlation: The Pearson correlation Coefficient is Superior to the Mander's Overlap Coefficient. Cytometry Part A *77A*, 733-742.

Anding, A.L., and Baehrecke, E.H. (2017). Cleaning House: Selective Autophagy of Organelles. Dev Cell *41*, 10-22.

Baens, M., Noels, H., Broeckx, V., Hagens, S., Fevery, S., Billiau, A.D., Vankelecom, H., and Marynen, P. (2006). The Dark Side of EGFP: Defective Polyubiquitination. PLOS ONE *1*, e54.

Bingol, B., Tea, J.S., Phu, L., Reichelt, M., Bakalarski, C.E., Song, Q., Foreman, O., Kirkpatrick, D.S., and Sheng, M. (2014). The mitochondrial deubiquitinase USP30 opposes parkin-mediated mitophagy. Nature *510*, 370-375.

Bottone, M.G., Santin, G., Aredia, F., Bernocchi, G., Pellicciari, C., and Scovassi, A.I. (2013). Morphological Features of Organelles during Apoptosis: An Overview. Cells *2*, 294-305.

Chernousova, S., and Epple, M. (2017). Live-cell imaging to compare the transfection and gene silencing efficiency of calcium phosphate nanoparticles and a liposomal transfection agent. Gene Ther *24*, 282-289.



doi:10.6342/NTU201704022

Chu, Y.P., Hung, Y.H., Chang, H.Y., and Yang, W.Y. (2017). Chapter Fourteen - Assays to Monitor Lysophagy. In Methods in Enzymology, J.M.B.-S.P. Lorenzo Galluzzi, and K. Guido, eds. (Academic Press), pp. 231-244.

Clague, M.J., Coulson, J.M., and Urbe, S. (2012). Cellular functions of the DUBs. J Cell Sci *125*, 277-286.

Colosimo, A., Goncz, K.K., Holmes, A.R., Kunzelmann, K., Novelli, G., Malone, R.W., Bennett, M.J., and Gruenert, D.C. (2000). Transfer and expression of foreign genes in mammalian cells. Biotechniques *29*, 314-318, 320-312, 324 passim.

Cornelissen, T., Haddad, D., Wauters, F., Van Humbeeck, C., Mandemakers, W., Koentjoro, B., Sue, C., Gevaert, K., De Strooper, B., Verstreken, P., *et al.* (2014). The deubiquitinase USP15 antagonizes Parkin-mediated mitochondrial ubiquitination and mitophagy. Human Molecular Genetics *23*, 5227-5242.

Dikic, I., and Bremm, A. (2014). DUBs counteract parkin for efficient mitophagy. The EMBO Journal *33*, 2442-2443.

Durcan, T.M., Tang, M.Y., Pérusse, J.R., Dashti, E.A., Aguileta, M.A., McLelland, G.L., Gros, P., Shaler, T.A., Faubert, D., Coulombe, B., *et al.* (2014). USP8 regulates mitophagy by removing K6-linked ubiquitin conjugates from parkin. The EMBO Journal *33*, 2473-2491.

Fabris, C., Valduga, G., Miotto, G., Borsetto, L., Jori, G., Garbisa, S., and Reddi, E. (2001).



doi:10.6342/NTU201704022

Photosensitization with Zinc (II) Phthalocyanine as a Switch in the Decision between Apoptosis and Necrosis. Cancer Research *61*, 7495-7500.

Galluzzi, L., Baehrecke, E.H., Ballabio, A., Boya, P., Bravo-San Pedro, J.M., Cecconi, F., Choi, A.M., Chu, C.T., Codogno, P., Colombo, M.I., *et al.* (2017). Molecular definitions of autophagy and related processes. EMBO J, 1-26.

Hsieh, C.W., Chu, C.H., Lee, H.M., and Yuan Yang, W. (2015). Triggering mitophagy with far-red fluorescent photosensitizers. Sci Rep *5*, 10376.

Hung, Y.-H., Chen, L.M.-W., Yang, J.-Y., and Yuan Yang, W. (2013). Spatiotemporally controlled induction of autophagy-mediated lysosome turnover. Nat Commun *4*.

Hunt, M.A., Currie, M.J., Robinson, B.A., and Dachs, G.U. (2010). Optimizing Transfection of Primary Human Umbilical Vein Endothelial Cells Using Commercially Available Chemical Transfection Reagents. Journal of Biomolecular Techniques : JBT *21*, 66-72.

Kabeya, Y., Mizushima, N., Ueno, T., Yamamoto, A., Kirisako, T., Noda, T., Kominami, E., Ohsumi, Y., and Yoshimori, T. (2000). LC3, a mammalian homologue of yeast Apg8p, is localized in autophagosome membranes after processing. The EMBO Journal *19*, 5720-5728.

Karbowski, M., and Youle, R.J. (2003). Dynamics of mitochondrial morphology in healthy cells and during apoptosis. Cell Death Differ *10*, 870-880.



doi:10.6342/NTU201704022

Keusekotten, K., Elliott, Paul R., Glockner, L., Fiil, Berthe K., Damgaard, Rune B., Kulathu, Y., Wauer, T., Hospenthal, Manuela K., Gyrd-Hansen, M., Krappmann, D., *et al.* (2013). OTULIN Antagonizes LUBAC Signaling by Specifically Hydrolyzing Met1-Linked Polyubiquitin. Cell *153*, 1312-1326.

Khaminets, A., Behl, C., and Dikic, I. (2015). Ubiquitin-Dependent And Independent Signals In Selective Autophagy. Trends in Cell Biology *26*, 6-16.

Kirkin, V., McEwan, D.G., Novak, I., and Dikic, I. (2009). A Role for Ubiquitin in Selective Autophagy. Molecular Cell *34*, 259-269.

Komander, D., Clague, M.J., and Urbe, S. (2009). Breaking the chains: structure and function of the deubiquitinases. Nat Rev Mol Cell Biol *10*, 550-563.

Kondapalli, C., Kazlauskaite, A., Zhang, N., Woodroof, H.I., Campbell, D.G., Gourlay, R., Burchell, L., Walden, H., Macartney, T.J., Deak, M., *et al.* (2012). PINK1 is activated by mitochondrial membrane potential depolarization and stimulates Parkin E3 ligase activity by phosphorylating Serine 65. Open Biol *2*, 120080.

Koyano, F., Okatsu, K., Kosako, H., Tamura, Y., Go, E., Kimura, M., Kimura, Y., Tsuchiya, H., Yoshihara, H., Hirokawa, T., *et al.* (2014). Ubiquitin is phosphorylated by PINK1 to activate parkin. Nature *510*, 162-166.

Kraft, C., Peter, M., and Hofmann, K. (2010). Selective autophagy: ubiquitin-mediated recognition and beyond. Nat Cell Biol *12*, 836-841.



doi:10.6342/NTU201704022

Lemasters, J.J. (2005). Selective Mitochondrial Autophagy, or Mitophagy, as a Targeted Defense Against Oxidative Stress, Mitochondrial Dysfunction, and Aging. Rejuvenation Research *8*, 3-5.

Li, L., Hailey, D.W., Soetandyo, N., Li, W., Lippincott-Schwartz, J., Shu, H.-b., and Ye, Y. (2008). Localization of A20 to a lysosome-associated compartment and its role in NFκB signaling. Biochimica et Biophysica Acta (BBA) - Molecular Cell Research *1783*, 1140-1149.

Liu, H.S., Jan, M.S., Chou, C.K., Chen, P.H., and Ke, N.J. (1999). Is green fluorescent protein toxic to the living cells? Biochemical and biophysical research communications *260*, 712-717.

Magraoui, F.E., Reidick, C., Meyer, H.E., and Platta, H.W. (2015). Autophagy-Related Deubiquitinating Enzymes Involved in Health and Disease. Cells *4*, 596-621.

Maurisse, R., De Semir, D., Emamekhoo, H., Bedayat, B., Abdolmohammadi, A., Parsi, H., and Gruenert, D.C. (2010). Comparative transfection of DNA into primary and transformed mammalian cells from different lineages. BMC Biotechnology *10*, 9.

Mei, Y., Hahn, A.A., Hu, S., and Yang, X. (2011). The USP19 Deubiquitinase Regulates the Stability of c-IAP1 and c-IAP2. Journal of Biological Chemistry *286*, 35380-35387.

Mevissen, Tycho E.T., Hospenthal, Manuela K., Geurink, Paul P., Elliott, Paul R., Akutsu, M., Arnaudo, N., Ekkebus, R., Kulathu, Y., Wauer, T., El Oualid, F., *et al.* (2013). OTU



doi:10.6342/NTU201704022

Deubiquitinases Reveal Mechanisms of Linkage Specificity and Enable Ubiquitin Chain Restriction Analysis. Cell *154*, 169-184.

Narendra, D., Tanaka, A., Suen, D.F., and Youle, R.J. (2008). Parkin is recruited selectively to impaired mitochondria and promotes their autophagy. J Cell Biol *183*, 795-803.

Nath, S., Dancourt, J., Shteyn, V., Puente, G., Fong, W.M., Nag, S., Bewersdorf, J., Yamamoto, A., Antonny, B., and Melia, T.J. (2014). Lipidation of the LC3/GABARAP family of autophagy proteins relies on a membrane-curvature-sensing domain in Atg3. Nat Cell Biol *16*, 415-424.

Nunnari, J., and Suomalainen, A. (2012). Mitochondria: In Sickness and in Health. Cell *148*, 1145-1159.

Okamoto, K. (2014). Organellophagy: Eliminating cellular building blocks via selective autophagy. The Journal of Cell Biology *205*, 435-445.

Okatsu, K., Uno, M., Koyano, F., Go, E., Kimura, M., Oka, T., Tanaka, K., and Matsuda, N. (2013). A Dimeric PINK1-containing Complex on Depolarized Mitochondria Stimulates Parkin Recruitment. Journal of Biological Chemistry *288*, 36372-36384.

Reyes-Turcu, F.E., Ventii, K.H., and Wilkinson, K.D. (2009). Regulation and Cellular Roles of Ubiquitin-Specific Deubiquitinating Enzymes. Annual Review of Biochemistry *78*, 363-397.



doi:10.6342/NTU201704022

Satoo, K., Noda, N.N., Kumeta, H., Fujioka, Y., Mizushima, N., Ohsumi, Y., and Inagaki, F. (2009). The structure of Atg4B–LC3 complex reveals the mechanism of LC3 processing and delipidation during autophagy. The EMBO Journal *28*, 1341-1350.

Shaid, S., Brandts, C.H., Serve, H., and Dikic, I. (2013). Ubiquitination and selective autophagy. Cell Death Differ *20*, 21-30.

Sowa, M.E., Bennett, E.J., Gygi, S.P., and Harper, J.W. (2009). Defining the Human Deubiquitinating Enzyme Interaction Landscape. Cell *138*, 389-403.

Taghizadeh, R.R., and Sherley, J.L. (2008). CFP and YFP, but not GFP, provide stable fluorescent marking of rat hepatic adult stem cells. J Biomed Biotechnol *2008*, 453590.

Tanida, I., Ueno, T., and Kominami, E. (2004). LC3 conjugation system in mammalian autophagy. The International Journal of Biochemistry & Cell Biology *36*, 2503-2518.

Tu, Z., He, G., Li, K.X., Chen, M.J., Chang, J., Chen, L., Yao, Q., Liu, D.P., Ye, H., Shi, J., *et al.* (2005). An improved system for competent cell preparation and high efficiency plasmid transformation using different Escherichia coli strains. Electronic Journal of Biotechnology *8*, 113-120.

Urbé, S., Liu, H., Hayes, S.D., Heride, C., Rigden, D.J., and Clague, M.J. (2012). Systematic survey of deubiquitinase localization identifies USP21 as a regulator of centrosome- and microtubule-associated functions. Molecular Biology of the Cell *23*, 1095-1103.



doi:10.6342/NTU201704022

Valente, E.M., Abou-Sleiman, P.M., Caputo, V., Muqit, M.M.K., Harvey, K., Gispert, S., Ali, Z., Del Turco, D., Bentivoglio, A.R., Healy, D.G., *et al.* (2004). Hereditary Early-Onset Parkinson's Disease Caused by Mutations in PINK1. Science *304*, 1158-1160.

Wang, Y., Serricchio, M., Jauregui, M., Shanbhag, R., Stoltz, T., Di Paolo, C.T., Kim, P.K., and McQuibban, G.A. (2015). Deubiquitinating enzymes regulate PARK2-mediated mitophagy. Autophagy *11*, 595-606.

Xie, Z., and Klionsky, D.J. (2007). Autophagosome formation: core machinery and adaptations. Nat Cell Biol *9*, 1102-1109.

Yang, J.H., Gross, R.L., Basinger, S.F., and Wu, S.M. (2001). Apoptotic cell death of cultured salamander photoreceptors induced by cccp: CsA-insensitive mitochondrial permeability transition. J Cell Sci *114*, 1655-1664.

Yang, J.Y., and Yang, W.Y. (2011). Spatiotemporally controlled initiation of Parkin-mediated mitophagy within single cells. Autophagy *7*, 1230-1238.

Ziegler, U., and Groscurth, P. (2004). Morphological Features of Cell Death. Physiology *19*, 124-128.



doi:10.6342/NTU201704022